

POTENTIAL IMPACTS OF CABLE BACTERIA ACTIVITY ON HARD-SHELLED BENTHIC FORAMINIFERA: ~~A PRELUDE TO~~ IMPLICATIONS FOR THEIR INTERPRETATION AS BIOINDICATORS OR PALEOPROXIES

Maxime Daviray^{1*}, Emmanuelle Geslin¹, Nils Risgaard-Petersen², Vincent V. Scholz³, Marie Fouet^{1,4},
Edouard Metzger¹

*Correspondence: Maxime DAVIRAY (maxime.daviray@univ-angers.fr)

¹ ~~Univ Angers, Nantes Université, Le Mans Université, CNRS, Laboratoire de Planétologie et Géosciences, LPG UMR 6112, 49000 Angers, France~~

~~⁴ UMR CNRS 6112 - LPG, Université d'Angers, Nantes Université, Le Mans Université, CNRS, 49000 Angers, France~~

² Aquatic Biology, Department of Biology, Aarhus University, 8000 Aarhus C, Denmark

³ Center for Electromicrobiology, Department of Biology, Aarhus University, 8000 Aarhus C, Denmark

⁴ at present: UMR CNRS 5805 EPOC - OASU, Station Marine d'Arcachon, Université de Bordeaux, CNRS, 33120 Arcachon, France

ABSTRACT

~~Cable bacteria (CB) are filamentous bacteria coupling sulphide oxidation to oxygen reduction over centimetre distances. This bacterial activity generates a strong pH gradient within the first few centimetres of the sediment that affects the microhabitats occupied by benthic foraminifera.~~ Hard-shelled foraminifera are protists able to build a calcareous or agglutinated shell (called "test"). Here we study the impact of sediment acidification **induced by CB activity (CBA)** on calcareous test preservation. For this study, sediment cores were sampled in the macrotidal Auray estuary located on the French Atlantic coast. Living and dead foraminifera were quantified (~~until 5-cm depth~~) and discriminated using the Cell-Tracker™ Green vital marker. ~~CBA was assessed with~~ pH and oxygen profiles combined with quantitative Polymerase Chain Reaction (q-PCR) **suggested that cable bacteria were most likely to cause the acidifying process.** ~~Cable bacteria (CB) are filamentous bacteria coupling sulphide oxidation to oxygen reduction over centimetre distances. This bacterial activity generates~~ **ing a strong pH gradient within the first few centimetres of the sediment that affects** ~~could affect the microhabitats occupied by benthic foraminifera.~~ On two different intertidal mudflats, volumetric filament densities have been ~~measured~~ **estimated**. They were comparable to those observed in the literature for coastal environments, with 7.4 ± 0.4 and 74.4 ± 5.0 m.cm⁻³ per bulk sediment respectively. Highly contrasting **sediment acidification** ~~CBA~~ (from low to very intense) were described **with from 1.0 to 2.4 ΔpH** ~~lowest pH at 5-8~~. This seems to lead to various dissolution stages of the foraminiferal calcareous test from intact to fully dissolved tests revealing the organic lining. The dissolution scale is based on observations of living *Ammonia* spp. and *Haynesina germanica* specimens under a Scanning Electronic Microscope. Furthermore, dead foraminiferal assemblages showed a strong calcareous test loss and an organic lining

37 accumulation throughout depth under low pH, hampering the test preservation in deep
38 sediment. These changes in both living and dead foraminiferal assemblages ~~imply-suggest~~
39 that ~~GB-cable bacteria~~ must be ~~strongly~~ considered in ecological monitoring and historical
40 studies using foraminifera as bioindicator and paleoenvironmental proxy.

41 1 INTRODUCTION

42 ~~Cable bacteria (CB) were discovered by Pfeffer and co-workers in 2012. They are sulphide-~~
43 ~~oxidizing filamentous multicellular prokaryotes from the Desulfobulbaceae family. They live in~~
44 ~~marine and freshwater sediments all around the world (Risgaard-Petersen et al., 2015; Burdorf~~
45 ~~et al., 2017). They inhabit a several centimetres thick zone from the oxic surface to the deep~~
46 ~~sulphidic sediment. CB generate a vertical bioelectrical current by coupling the cathodic~~
47 ~~oxygen or nitrate reduction at the sediment surface to the anodic sulphide oxidation at depth~~
48 ~~(Nielsen et al., 2010; Pfeffer et al., 2012; Risgaard-Petersen et al., 2012; Marzocchi et al.,~~
49 ~~2014). CB activity (CBA) strongly affects sediment geochemistry and results in a clear~~
50 ~~geochemical fingerprint: an oxygen decrease in the surface sediments combined with a pH~~
51 ~~maximum in this oxic zone, followed by a strong acidification of the pore water in the suboxic~~
52 ~~zone (Nielsen et al., 2010; Risgaard-Petersen et al., 2012, 2014; Moysman et al., 2015). It~~
53 ~~leads to iron sulphide and carbonate dissolution from the suboxic zone (Risgaard-Petersen et~~
54 ~~al., 2012; Rao et al., 2016; van de Velde et al., 2016) and possibly the calcareous shell of~~
55 ~~benthic organisms.~~

56 Benthic foraminifera are unicellular meiofaunal organisms. Most species can build a hard-shell
57 (called a test) that can be agglutinated (cemented grains), hyaline calcareous (calcium
58 carbonate) and porcelaneous calcareous (calcium carbonate enriched in magnesium). Benthic
59 foraminifera are very abundant in marine areas (Martin, 2000) including transitional
60 environments (Alve & Murray, 1999; Debenay et al., 2006). These systems located between
61 marine and continental areas (i.e. littoral and estuarine zones), are subjected to a high
62 variability of environmental factors (e. g. tide, freshwater flows, evaporation, development of
63 seagrass meadows over seasonal cycles...). Then, benthic foraminifera are submitted to
64 strong variability of physical and geochemical parameters such as temperature, salinity or pH
65 that they must tolerate. Despite such variability, benthic foraminifera assemblages have been
66 used in transitional environments as bioindicators for biomonitoring ecological state and ~~as~~
67 assemblages and chemical test composition as paleoenvironmental proxies to understand
68 past ecosystems functioning (Martin, 2000; Murray, 2006; Katz et al., 2010; Keul et al., 2017;
69 Durand et al., 2018). However, species with a calcareous test can be affected by ~~low~~
70 pH sediment acidification and carbonate undersaturation leading to test dissolution (Le Cadre
71 et al., 2003; Bentov et al., 2009; de Nooijer et al., 2009; Haynert et al., 2011, 2014; Kurtarkar
72 et al., 2011; Charrieau et al., 2018b). Even if they are rarely observed *in situ*, few studies have
73 reported signs of severe test dissolution in living assemblages (e.g., Alve and Nagy, 1986;
74 Buzas-Stephens, 2005; Polovodova and Schonfeld, 2008; Haynert et al., 2012; Cesbron et al.,
75 2016; Charrieau et al., 2018a; Schönfeld and Mendes, 2022). These authors attribute these
76 dissolution observations to low pH and undersaturation of the carbonate system, which would

77 be due to abiotic conditions (anthropogenic pollution, freshwater intrusions) or more rarely to
78 biotic ones (degradation of plants). Under laboratory conditions, Le Cadre et al. (2003) have
79 shown that test dissolution of living *Ammonia beccarii* starts at pH 7.0 after five days and can
80 recalcify in standard conditions after eight days. Charrieau et al. (2018c) have shown that
81 *Elphidium crispum* decalcified earlier than *Ammonia* sp. under seawater acidification
82 (respectively nine and 30 days at pH~7.25). These authors also showed that test dissolution
83 occurred even more prematurely in brackish waters (before nine days at pH≤7.53).

84 Sediment acidification may be link to cable bacteria activity. Cable bacteria (CB) were
85 discovered by Pfeffer and co-workers in 2012. They are sulphide-oxidizing filamentous
86 multicellular procaryotes from the Desulfobulbaceae family. They live in marine and freshwater
87 sediments all around the world (Risgaard-Petersen et al., 2015; Burdorf et al., 2017). They
88 inhabit a several centimetres thick zone from the oxic surface to the deep sulphidic sediment.
89 CB generate a vertical bioelectrical current by coupling the cathodic oxygen or nitrate reduction
90 at the sediment surface to the anodic sulphide oxidation at depth (Nielsen et al., 2010; Pfeffer
91 et al., 2012; Risgaard-Petersen et al., 2012; Marzocchi et al., 2014). CB activity (CBA) strongly
92 affects sediment geochemistry and results in a clear geochemical fingerprint: an oxygen
93 decrease in the surface sediments combined with a pH maximum in this oxic zone, followed
94 by a strong acidification of the pore water in the suboxic zone (Nielsen et al., 2010; Risgaard-
95 Petersen et al., 2012, 2014; Meysman et al., 2015). It leads to iron sulphide and carbonate
96 dissolution from the suboxic zone (Risgaard-Petersen et al., 2012; Rao et al., 2016; van de
97 Velde et al., 2016) and possibly the calcareous shell of benthic organisms.

98

99 Benthic foraminifera live mainly in the topmost sediment. CB-cable bacteria develop
100 also on the few topmost centimetres of the sediment, which can therefore lead to an
101 environmental overlap of the bacterial and foraminiferal communities. Richirt et al 2022
102 hypothesised that CBA induces-could induce the dissolution of calcareous tests within the
103 sediment of the Lake Grevelingen (Netherlands). In the present study, we assess the impact
104 of cable bacteria activity on the foraminiferal test preservation in sediment, testing the
105 hypothesis that CBA-cable bacteria activity is responsible for depleting the preservation of
106 calcareous foraminifera in benthic assemblages. To achieve this, CBA was characterized by
107 oxygen and pH microprofiling and CB density quantified by qPCR on intertidal mudflats of the
108 Auray estuary (French Atlantic coast). Foraminiferal calcareous test dissolution stages were
109 defined and quantified thanks to the analyse of SEM images. Then, we described living and
110 dead foraminiferal assemblages to assess the calcareous test loss.

111 **2 MATERIALS AND METHODS**

112 **2.1 Studied Area**

113 The Gulf of Morbihan (Atlantic coast, France) is an enclosed marine bay where the Auray river
114 flows. The Auray estuary is a macrotidal estuary with a tide range about 4 m (**Figure 1**).

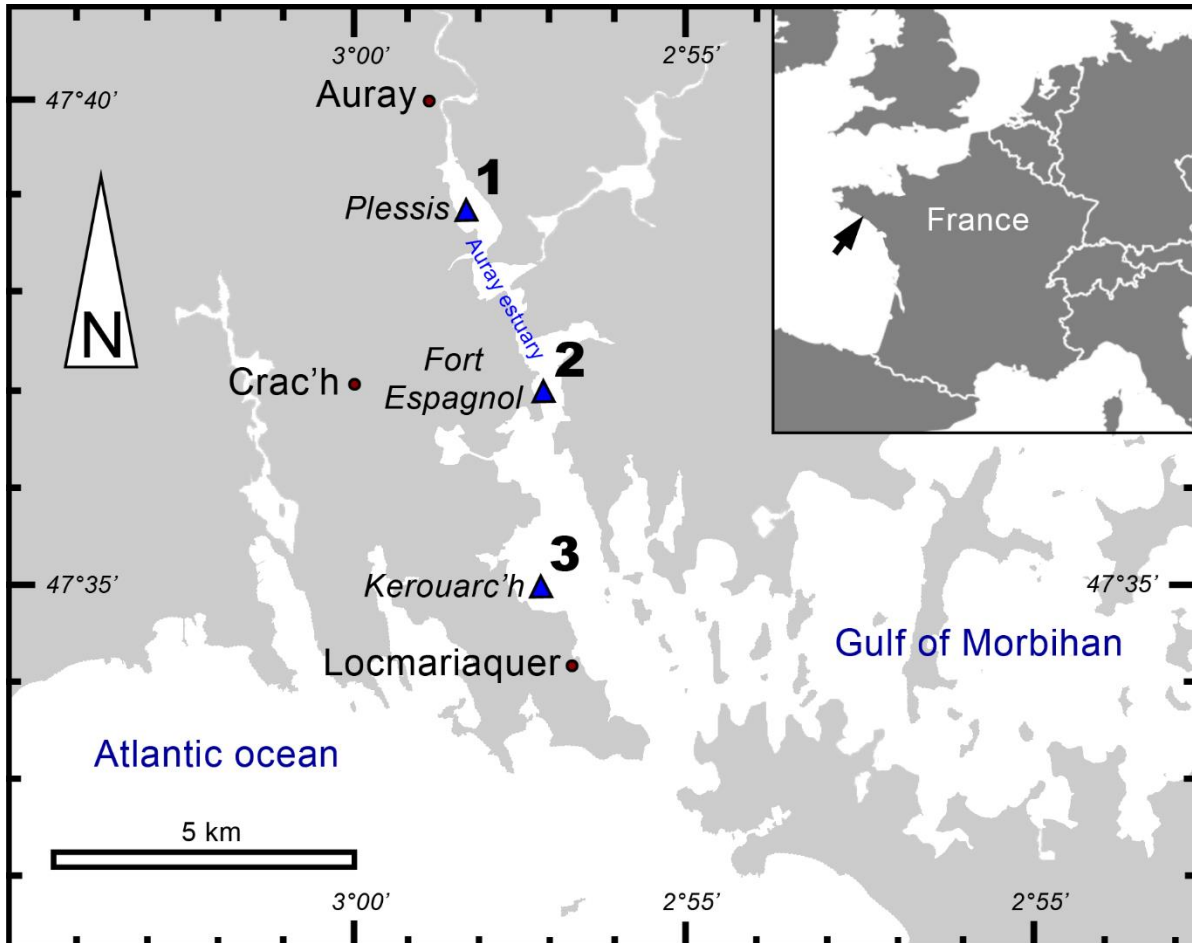


Figure 1. Locations of sampling stations in the intertidal mudflats of the Auray estuary (France).

115 Saltwater flows upstream over 20 km from the mouth of the estuary (357 m wide) which is tide-
116 dominated (online data from [OFB](#) and [IFREMER](#), accessed on May 05th 2022). The extensive
117 description of this area was (e.g. the marine influence, hydrodynamics and granulometry) has
118 been reported made by Fouet et al. (2022).

119 In September 2020, three stations along the Auray estuary were sampled on intertidal
120 mudflats at low tide (**Figure 1** and **Table 1**): station 1 (Plessis), station 2 (Fort Espagnol) and
121 stations 3 (Kerouarc'h). Characteristics of the sampled stations are presented in **Table 1**.

122 **Table 1. Characteristics of the stations sampled in September 2020.** Temperature and salinity values
 123 correspond to these measured on the sampling day; weighted average and SD of sediment density data from a
 124 previous campaign in 2019; (*) name of the station after Fouet et al., (2022).

STATION	COORDINATES	DISTANCE FROM SEA	T (°C)	SALINITY	SEDIMENT DENSITY (g.cm ⁻³)	VEGETATION COVER
1 (*6B)	47.646° N, -2.972° W	12 km	24.4	29.6	1.71 ± 0.12	<i>Ulvea</i> mat
2 (*4B)	47.616° N, -2.953° W	8 km	21.2	38.5	1.67 ± 0.33	<i>Ulvea</i> mat
3 (*2C)	47.583° N, -2.955° W	4.3 km	21.5	34.3	1.51 ± 0.23	thick <i>Ulvea</i> mat few <i>Zostera</i>

125 2.2 Sediment Sampling and Processing

126 One core was sampled from each station by hand with a Plexiglas® tube (82 mm inner
 127 diameter, 50 mm depth) and was transported within an hour in a cool box to the field laboratory.
 128 Then, the cores were submerged in ambient seawater for at least two hours to retrieve *in situ*
 129 conditions before microprofiling.

130 After microprofiling, each core was sliced using a core pusher and two trowels. Slice
 131 thickness was 2 mm for the first 20 mm depth, and 10 mm up to 50 mm depth. Each sediment
 132 slice was treated with Cell-Tracker™ Green (CTG 5 CMFDA: 5-chloromethylfluorescein
 133 diacetate; Molecular Probes, Invitrogen Detection Technologies) to mark living benthic
 134 foraminifera by fluorescence (Bernhard and Bowser, 1996; Bernhard et al., 2006). One mg of
 135 CTG was dissolved in 1 mL of dimethylsulfoxide (DMSO). This solution was then pipetted into
 136 the flask containing the sediment slice and its volume of ambient water to get a final solution
 137 of CTG about 1 µM (Bernhard et al., 2006; Pucci et al., 2009; Langlet et al., 2013, 2014;
 138 Cesbron et al., 2016). Each sample was then incubated in dark at room temperature overnight
 139 and then fixed with ethanol 99% (Choquel et al., 2021). Eventually, the samples were **quickly**
 140 **and gently** sieved with tap water over 315-, 150-, 125- and 63-µm mesh screens. Samples
 141 were conserved in 99% ethanol.

142 DNA was extracted from sub-samples of sediment slices at stations 1 and 2. 1-2 g
 143 every second slice down to 18-mm depth were sampled with a heat-sterilized spatula and
 144 transferred to 2 ml Eppendorf tubes, then frozen at -20°C degrees. Samples were sent in dry
 145 ice (CO_{2(s)} at -50°C) to the Microbiology Institute of Biology in Aarhus University (Denmark) for
 146 qPCR analysis to quantify cable bacteria biomass.

147 2.3 Microsensor Profiling

148 Two Unisense© profiling systems were used simultaneously. One consisted of two oxygen
 149 Clark-type microsensors with a 50-µm **diameter** tip (Revsbech and Jørgensen, 1986;

150 Revsbech, 1989), and the other of a pH sensor with a 500 μm tip diameter (PH500, Unisense).
151 They were both mounted on a motorized micromanipulator linked to a computer, and
152 connected to a MultiMeter S/N. The increment was 50 μm until 3 mm for oxygen. It was 100
153 μm around the seawater-sediment interface (SWI) for pH, and it was adapted in real time
154 according to the evolution of the observed profile until 50 mm depth. For each core, eight
155 descents were managed for O_2 , for a total of 16 profiles, while ~~only~~ one profiling was done for
156 pH. To calibrate the O_2 microsensor, two points were measured, with the 100% of oxygen
157 saturation in the bubbling seawater column, and the 0% into the anoxic part of sediment. To
158 calibrate the pH microsensor, 3 NBS buffers were used (values 4.0, 7.0, 9.2).

159 **2.4 Living Foraminiferal Analyses**

160 Counts of hard-shell benthic foraminifera were performed in wet conditions (water) on the >125
161 μm fractions using an epifluorescence stereomicroscope (Olympus SZX12 with a light source
162 CoolLED pE-100, emission wavelength $\lambda = 470 \text{ nm}$). All specimens showing clear green
163 fluorescence were picked and identified. Remaining specimens were considered as dead. In
164 doubtful cases, particularly with agglutinated species, specimens were crushed to inspect
165 whether fluorescence was due to the presence of protoplasm, to the autofluorescence of
166 sediment grains composing the test, or the presence of bacteria or nematodes living inside
167 (Langlet et al., 2013; Cesbron et al., 2016). Total foraminiferal densities were expressed per
168 50 cm^2 of sediment and foraminiferal densities for sediment layers per 10 cm^3 volume.

169 For the taxonomy of hard-shell foraminifera species, reference publications on
170 estuarine foraminifera (Feyling-Hanssen et al, 1972; Hansen et al, 1976; Murray et al, 1979;
171 Scott et al, 1980; Hayward et al, 2004; Schweizer et al, 2011; Camacho et al, 2015; Richirt et
172 al, 2019; Fouet et al., 2022; Jorissen et al., 2023), and the World Register of Marine Species
173 were used. The distinction between the *Ammonia* phylotypes (Richirt et al, 2019) being difficult,
174 on particular on the dissolved tests, the results will be discussed at the genus level.

175 **2.5 SEM Imaging**

176 Living foraminifera from three layers (0-2 / 6-8 / 40-50 mm depth), according to main pH
177 features, were all observed under a Scanning Electronic Microscope (SEM). Two different
178 high-resolution SEM were used: a DEBEN Hitachi TM4000 at the LPG (samples not
179 metallised, 15kV, wd = 6,5 mm, partial vacuum (60 Pa)) and a Zeiss EVO LS10 at the Service
180 Commun d'Imageries et d'Analyses Microscopiques of Angers University (SCIAM; samples
181 not metallised, 20 kV, wd = 6,5 mm, partial vacuum (60 Pa), amperage 200 to 250 pA). Few
182 scales of calcareous test dissolution of living foraminifera have been proposed in the literature
183 (Corliss and Honjo, 1981; Le Cadre, 2003b; Haynert et al., 2011; Gonzales et al., 2017;
184 Charrieau et al., 2018c, [2022](#); Schönfeld and Mendes, 2022). These authors proposed scales

185 varying from 4 to 5 different stages based on SEM images or stereomicroscope observations.
 186 They used a wide variety of morphological criteria to describe each dissolution stage (i.e. the
 187 number of calcite layers altered and chambers damaged, the presence of cracks or holes,
 188 whether the inner organic lining was visible, etc.). In the present study, we propose a scale of
 189 six dissolution stages based on SEM pictures of the two most abundant calcareous species in
 190 our living assemblages (*Ammonia* spp. and *Haynesina germanica*).

191 **Table 2. Description of the six dissolution stages of the calcareous tests of *Ammonia* spp. and *Haynesina***
 192 ***germanica*.**

DISSOLUTION STAGE	NAME	SEM OBSERVATIONS AND STAGE DESCRIPTIONS	FIGURES
DS-0	Intact test	intact, glassy test with a smooth surface and cylindrical pores, no sign of dissolution.	Fig. 3-1 Fig. 4-1
DS-1	Slight surface dissolved test	transparent test with cylindrical pores, alteration of the last calcite layer only, appearance of the interpore sutures in <i>H. germanica</i> (scarce in <i>Ammonia</i> spp., alteration more visible on the inter-chamber walls).	Fig. 3-2 Fig. 4-2
DS-2	Peeled test	dull, whitish test with some fusion of adjacent widen pores, calcite layers cracking and crumbling, last chamber often lost, thinner and blunt tubercular ornamentation of <i>H. germanica</i> .	Fig. 3-3 Fig. 4-3
DS-3	Cracked test	opaque and cracked test with a strong alteration of all calcite layers, brittle test with holes, fusion of widen pores, the organic lining can be visible, loos of last chamber, broken ornamentation of <i>H. germanica</i> .	Fig. 3-4 Fig. 4-4
DS-4	“Star-shape” test	nearly completely dissolved test, only the inter-chamber walls remaining, the last chambers often absent, dissolved peripheral chambers with the inner organic lining visible.	Fig. 3-5 Fig. 4-5
DS-5	Fully dissolved test	totally dissolved test revealing the inner organic lining, may keep the foraminifera shape allowing the identification of the genus <i>Ammonia</i> (not observed for <i>H. germanica</i>).	Fig. 3-6

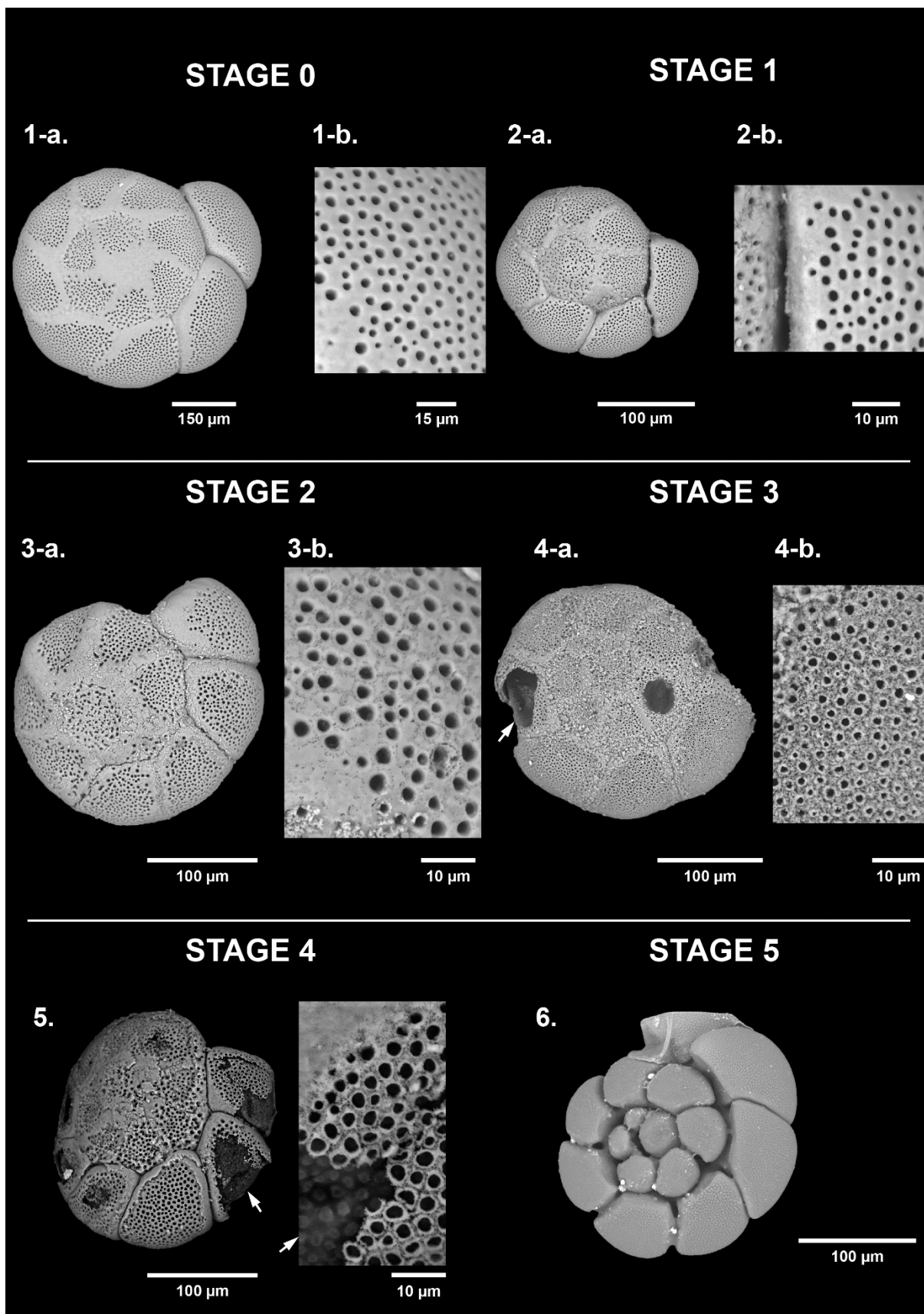


Figure 2. Dissolution scale of *Ammonia* spp. based on high-resolution SEM images (spiral view). The specimens are classified into six stages of test dissolution from intact (stage 0) to fully dissolved (stage 5). For stages 0 to 2, a zoom on the last formed chamber was done (1-b, 2-b, 3-b), and on the $n-1$ chamber for stage 3 (4-b). White arrows point the organic lining.

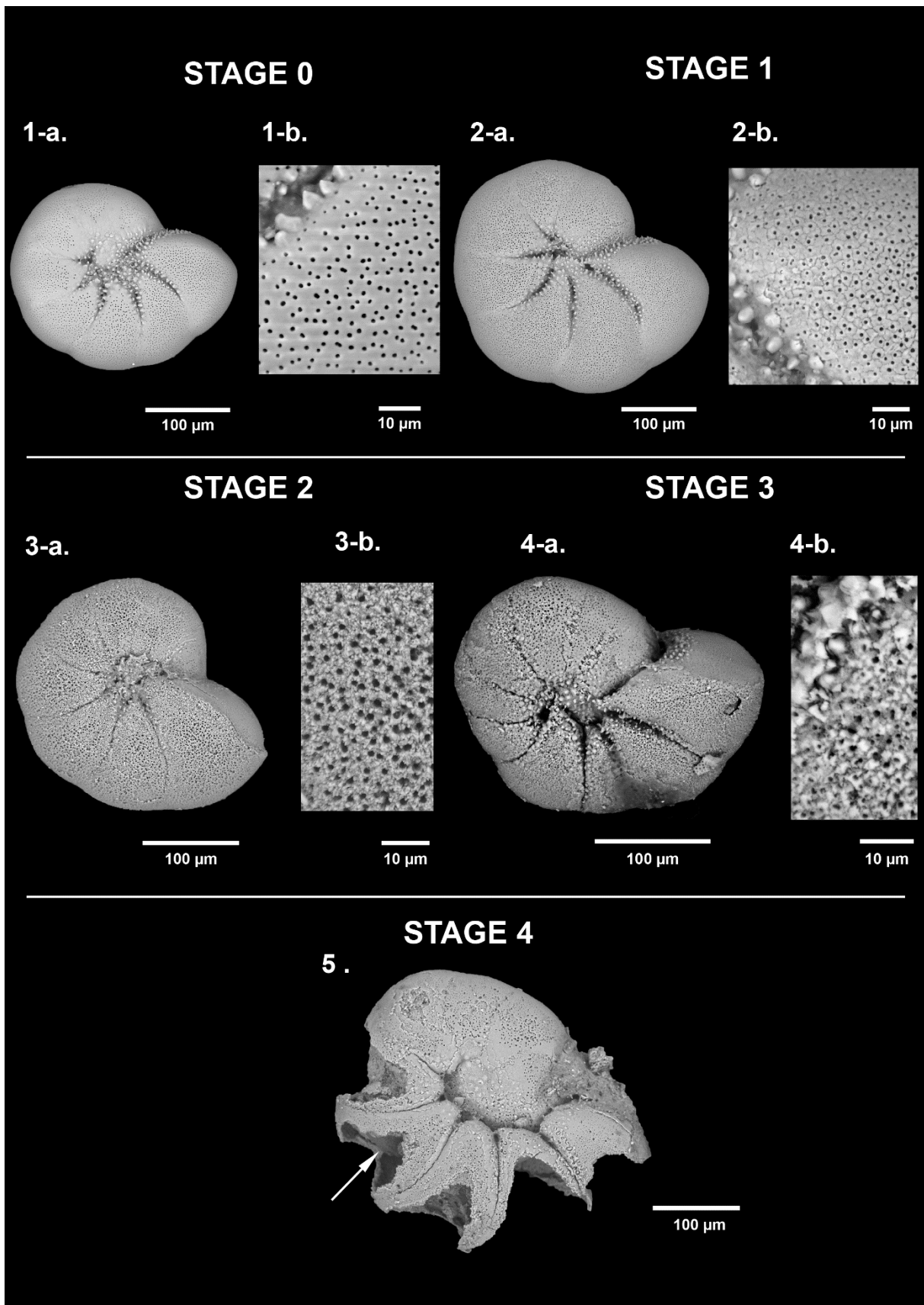


Figure 3. Dissolution scale of *Haynesina germanica* based on high-resolution SEM images. The specimens are classified into five stages of test dissolution from intact (stage 0) to the « star shape » (stage 4). No organic lining (stage 5) has been identified as belonging to the taxa *Haynesina*. For stages 0 and 1, a zoom on the last formed chamber was done (1-b, 2-b), and on the n-1 chamber for stages 2 and 3 (3-b, 4-b). White arrow points the organic lining.

195 **2.6 Dead Foraminiferal Analyses**

196 Non fluorescent tests of foraminifera were counted as dead specimens and picked in wet
197 conditions (water) to preserve the organic linings from fully dissolved tests. We proceeded
198 under a stereomicroscope (ZEISS Stemi sv11) in three sediment layers: the surface layer (0-
199 2 mm), the subsurface layer (6-8 mm) and the deep layer (40-50 mm). After quick observations,
200 when high densities were estimated (above 500 individuals; Patterson and Fishbein, (1989))
201 fractions were splitted into 8 sub-samples using a wet splitter (Charrieau et al., 2018a).

202 **2.7 Ratios in Foraminiferal Assemblages**

203 In order to characterize the loss of calcareous specimens in the assemblages, we defined a
204 ratio enabling each sample to be compared as follows:

$$205 \quad C/T = \text{calcareous foraminifera} / \text{total foraminifera}$$

206 Calcareous foraminifera are counted regardless their dissolution stage and total
207 foraminifera include agglutinated individuals. To estimate the intensity of dissolution in the
208 assemblage, we calculated the following ratio:

$$209 \quad DS-5/C = \text{calcareous test at dissolution stage 5} / \text{total calcareous foraminifera}$$

210 These ratios were calculated on both living and dead assemblages for layers 0-2 / 6-8
211 and 40-50 mm.

212 **2.8 Statistical Procedure**

213 The putative relationship between CBA—cable bacteria activity and the advanced dissolution
214 stages of the living calcareous test foraminifera was assessed by applying the parametric
215 Fisher's test followed by the pair-wise Fisher's test for *post-hoc* comparisons were used. To
216 minimize the risk type 1 error *p*-values were FDR-adjusted. The significance level was set to 5
217 %. As the last layer of calcite produced during the growth of the foraminifera covers the entire
218 test and is thinner than the others (Haynes, 1981; Hansen, 1999; Debenay et al., 2000;
219 Boudagher-Fadel, 2018), DS-1 and 2 are more commonly observed resulting from a process
220 of gradual dissolution or precipitation of calcite. Discrimination of the effect of the dissolution
221 process is therefore made on the alteration of several calcite layers as for DS-3 and above.
222 For this purpose, the dissolution stages were combined into two groups: no to slight dissolution
223 (DS-0, 1 and 2) and moderate to severe dissolution (DS-3, 4 and 5). These two groups were
224 then compared between each of the three stations, and between the different depth levels (0-
225 2 / 6-8 / 40-50 mm depth) for each station. Statistics were carried out using the *R* software
226 using the "stats" and "rstatix" packages.

227 **2.9 Sediment Treatment for DNA Extraction and Quantification**

228 DNA was extracted from weighed amounts of sediment (0.22 - 0.25 g wet weight). DNA
229 extraction was carried out using DNeasy PowerLyzer PowerSoil Kit (Qiagen) and the DNA was
230 collected in 60 µl elution buffer. The analysis followed the procedures outlined in Geelhoed et
231 al. (2020). The primer combination of ELF645wF and CB836wR was used to target the 16S
232 rRNA gene of the marine cable bacteria of the genus *Candidatus Electrothrix Trojan*, 2016.
233 The calibration curves were obtained using a synthetic standard (sequence accession
234 KR912339.1, position 611-912, synthesized by Eurofins Genomics, Denmark) diluted in a 10-
235 fold dilution series. The standards and samples were run in triplicates. Each reaction contained
236 the master mix (RealQ Plus 2x Master Mix Green, Low ROXTM, Ampliqon, Denmark), forward
237 and reverse primers (0.2 µM), BSA (1 µM). The qPCR was performed with a real time PCR
238 analyser (AriaMX, Agilent). The thermal cycles were as follows: 15 min at 95 °C for initial
239 denaturation followed by 40 cycles of 15 s at 95 °C (denaturation), 30 s at 60 °C (annealing),
240 and 20 s at 72 °C (amplification). Afterwards, the melting curve was obtained by 30 s at 95°C,
241 30 s at 60 °C, and 30 s at 95 °C. Finally, the temperature was held for 5 min at 40 °C to
242 terminate the analysis. The results are reported as the unit gene copies.(g wet sediment)⁻¹.
243 CB filament density were calculated as in Geelhoed et al. (2020), using data of wet sediment
244 density from a previous campaign in 2019 (**Table 1**), and expressed in m.cm⁻³. For
245 administrative reasons, it was only possible to carry out these DNA analyses for stations 1 and
246 2.

247 **3 RESULTS**

248 **3.1 Microsensor Profiles and Cable Bacteria Abundance**

249 Oxygen penetration depth in the sediment at stations 1, 2 and 3 was 1.4 ± 0.2, 0.9 ± 0.3 and
250 0.9 ± 0.2 mm, respectively. At station 1, pH rapidly decreased from 7.7 at the Sea Water
251 Interface (SWI) to a minimum of 6.8 at 15 mm depth. Below this minimum, pH stabilised to 7.2
252 around 40 mm depth. In contrast, at stations 2 and 3, pH increased immediately below the SWI
253 from 7.8 to 8.1 at 0.8 mm depth and to 7.95 at 0.6 mm, respectively (**Figure 4**). Below these
254 maxima, at both stations, pH reached a minimum of 5.8 at 7 mm depth at station 2 and of 6.3
255 between 7-19 mm depth at station 3. Below these minima, pH stabilised at 6.8 after 25 mm
256 depth at station 2, and at 6.9 after 34 mm depth at station 3. ~~These profiles with an oxygen~~
257 ~~decrease in the surface sediments combined with a pH maximum in this oxic zone, followed~~
258 ~~by a strong acidification of the pore water in the suboxic zone, are typical CBA fingerprints.~~

259 At station 1, the number of 16S CB copies of *Candidatus Electrothrix* ranged from 0.23
260 ± 0.01 ×10⁷ to 0.48 ± 0.01 ×10⁷ 16S copies.(g wet sediment)⁻¹, and remained constant through

261 depth (**Figure 4**). At station 2, it amounted to $2.8 \pm 0.12 \times 10^7$ 16S copies.(g wet sediment)⁻¹ in
 262 the upper 5 mm of sediment and progressively decreased to about $0.3 \pm 0.01 \times 10^7$ 16S
 263 copies.(g wet sediment)⁻¹ in the 16-18 mm depth layer. The maximum 16S CB copies of *Ca.*
 264 *Electrothrix* in station 2 corresponded to the maximum pH in depth. According to
 265 [GelhoodGeelhood](#) et al. (2020) and using wet sediment density from the same stations
 266 obtained in 2019 (pers. comm. M. Fouet), we calculated a CB-filament density of 7.4 ± 0.4 and
 267 74.4 ± 5.0 m.cm⁻³ at stations 1 and 2 respectively.

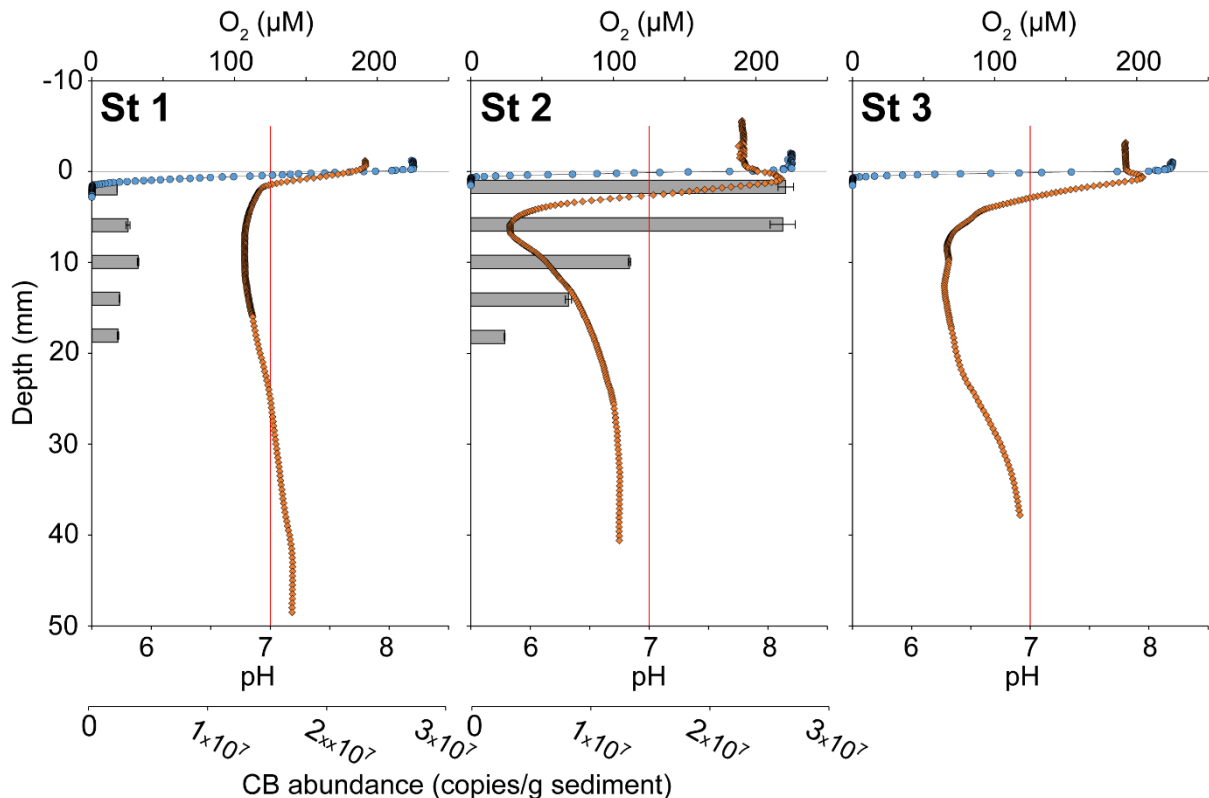


Figure 4. Sediment oxygen (blue circles) and pH (orange diamonds) microprofiles at the three stations, and vertical distribution of cable bacteria abundance (qPCR of *Ca. Electrothrix* 16S rRNA gene copies, grey bars) for stations 1 and 2. 0 is the position of the Sea Water Interface (SWI). The vertical red line represents neutral pH. The oxygen profile presented is one of those obtained by microprofiling, and representative of O₂ penetration for each station.

268 3.2 Hard-Shellled Benthic Foraminiferal

269 3.2.1 Living Foraminiferal Diversities and Densities

270 The foraminiferal species assemblages were typical of the estuarine environments (Debenay
 271 et al., 2000), with a poor species richness (14, 13 and 18 species at stations 1, 2 and 3
 272 respectively). *Ammonia* spp. and *Haynesina germanica* (Ehrenberg, 1840) both strongly
 273 dominated the assemblages at all three stations (25.1 and 51.5 % respectively of the total
 274 assemblage for station 1, 14.5 and 48.2 % for station 2, 7.3 and 61.4% for station 3; **Figure**
 275 **5**). *Ammonia* spp. included the species *Ammonia veneta* (Schultze, 1854) (phylotype T1 after
 276 Hayward et al., 2004), *Ammonia aberdoveyensis* Haynes, 1973 (phylotype T2 after Hayward
 277 et al., 2004), and *Ammonia confertitesta* Zheng, 1978 (phylotype T6 after Hayward et al.,

278 2004). Agglutinated foraminifera represent 19.9, 25.7 and 12.7 % of the total assemblage at
 279 stations 1, 2 and 3, respectively. They were dominated by *Ammobaculites agglutinans*

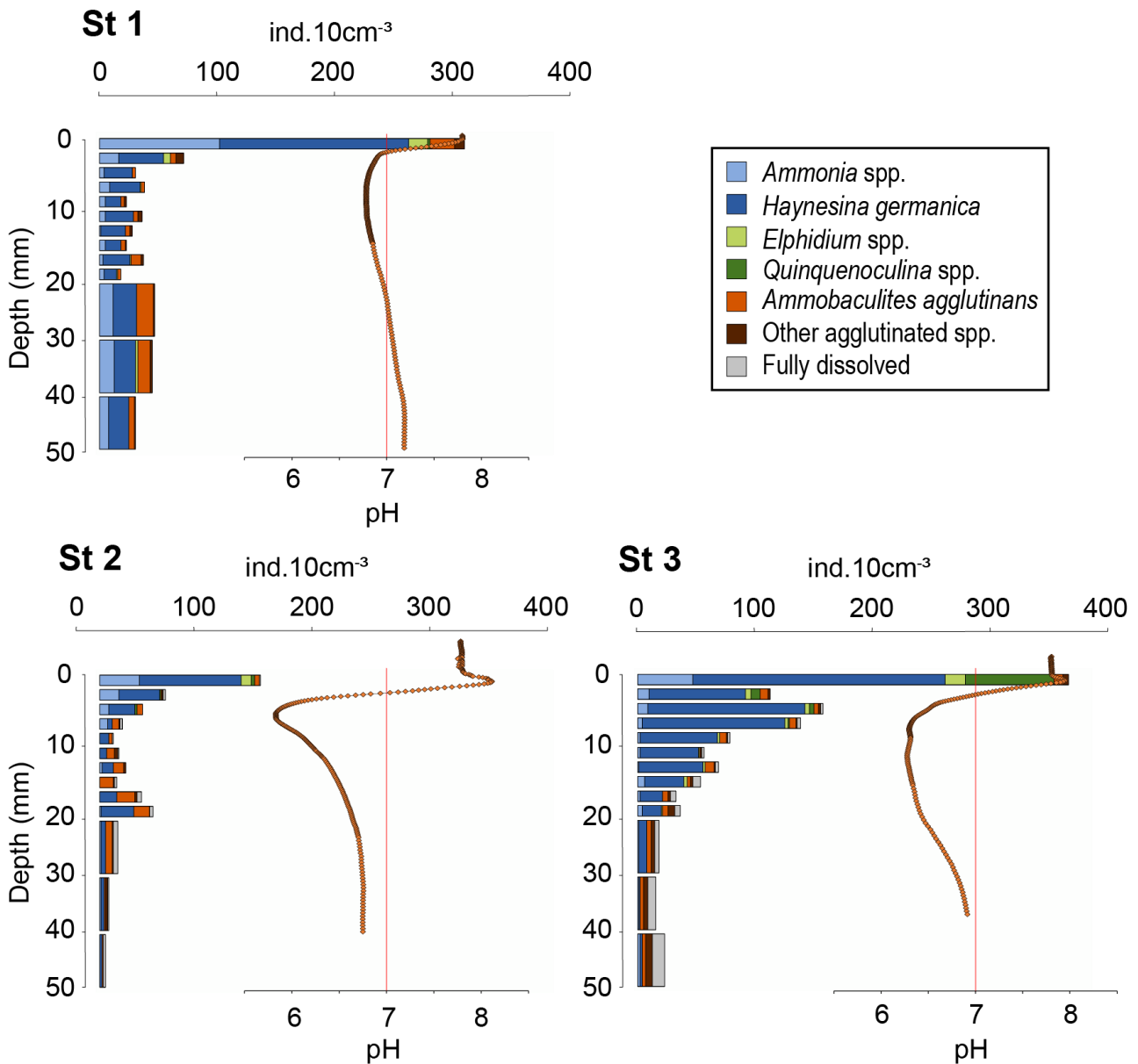


Figure 5. Vertical distributions of living-foraminifera densities per 10 cm³ of sediment at the three stations (>125 μ m fraction). 0 is the position of the Sea Water Interface (SWI). Recall of pH microprofiles (orange diamonds) and neutral pH (vertical red line).

280 (d'Orbigny, 1846).

281 3.2.2 Living Foraminiferal Vertical Distribution

282 Total densities of CTG-labelled foraminifera in cores 1, 2 and 3 were 1273, 548, and 1431
 283 ind.50cm⁻² respectively. Highest densities were found in the first layer of sediment (0-2 mm
 284 depth) for all cores with 295, 137 and 371 ind.10cm⁻³ at stations 1, 2 and 3, respectively (**Figure**
 285 **5**), where dioxygen was available and pH was maximal (**Figure 4**).

286 At station 1, total density dropped below 2 mm to stabilize at $30 \pm 9 \text{ ind.}10\text{cm}^{-3}$ (**Figure**
 287 **5**). At station 2, the vertical distribution of total densities showed two maxima. The first at the
 288 SWI and a second at 18-20 mm depth with $47 \text{ ind.}10\text{cm}^{-3}$. A first minimum of $11 \text{ ind.}10\text{cm}^{-3}$
 289 was observed at 8-10mm depth close to the lowest pH layer and a second minimum of 5
 290 $\text{ind.}10\text{cm}^{-3}$ was observed at the bottom of the core. At station 3, after a maximum at the SWI,
 291 foraminifera density decreased gradually with depth, following the pH trend, to reach on
 292 average $19 \pm 4 \text{ ind.}10\text{cm}^{-3}$ from 20 to 50 mm depth.

293 At station 1, the ratio of calcareous foraminifera in the living foraminiferal assemblage
 294 (C/T) was 0.91 for the SWI (**Table 3**) and around 0.77 ± 0.07 for the layers below. At station
 295 2, C/T was 0.97 of the SWI and on average 0.64 ± 0.16 between 2- and 50-mm depth
 296 (**Appendix**). However, agglutinated taxa dominated the assemblages from 10 to 18 mm, just
 297 below the pH minimum, with a drop of C/T ratio to 0.39 ± 0.18 (**Appendix**). At station 3, the
 298 C/T ratio was 0.97 at the SWI and decreased asymptotically as calcareous foraminiferal
 299 densities vanished to reach 0.72 ± 0.15 below 20 mm after the pH minimum zone (**Appendix**).

300 3.2.3 Calcareous Test Dissolution of Living Foraminifera

301 **Figure 6** shows the dissolution stage (DS) of calcareous foraminifera for three selected
 302 sediment layers (0-2 / 6-8 / 40-50 mm) for living assemblages. At station 1, living specimens
 303 with calcareous test showed low alteration. The DS remained stable through depth ($p > 0.05$).
 304 Specimens with “Intact tests” (DS-0) or “slight surface dissolved tests” (DS-1) represented 90
 305 % of calcareous foraminifera. The strongest dissolution stages were DS-2 (“peeled test”) and
 306 DS-3 (“cracked test”) accounting for less than 10 %.

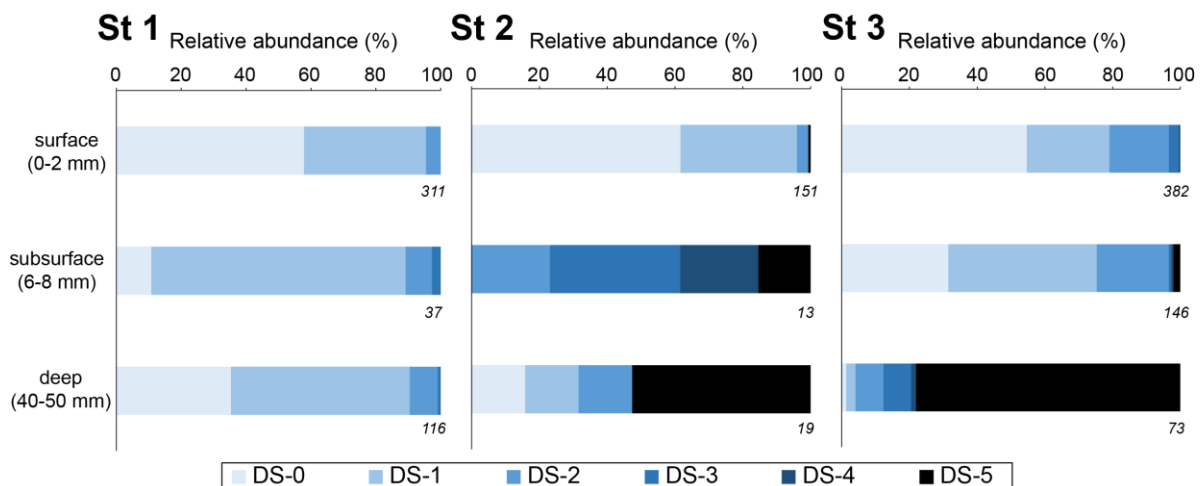


Figure 6. Relative abundance of living benthic foraminifera with calcareous test for each dissolution stage for 10 cm³ of sediment (*Ammonia* spp. and *H. germanica* from the >125 μm fraction). Three depth levels were analysed: the surface (0-2 mm; oxic zone), the subsurface (6-8 mm; suboxic zone corresponding to pH minimum), and the deeper (40-50 mm; anoxic zone). The numbers on the lower right of the boxes are the total numbers of SEM photographed specimens.

307 Conversely, at station 2, many foraminifera were very fragile under manipulation.
 308 Numerous “fully dissolved tests” (DS 5) with only the organic lining were observed through

309 depth (50 ind.50cm⁻²; **Appendix**). At the SWI (0-2 mm layer), DS-0 and DS-1 tests represented
310 95% of the calcareous test foraminifera in the living assemblage. Only few DS-2 and DS-5
311 specimens were present. In the subsurface level (6-8-mm depth), corresponding to the most
312 acidic conditions, no DS-0 and DS-1 specimen ~~were~~was observed. DS-4 and DS-5 tests were
313 about 40 % of the calcareous tests observed. At the deepest layer (40-50 mm), DS-5
314 specimens were dominant (>50 %). The surface layer was significantly different ($p < 0.005$)
315 from the two deeper layers that showed no significant differences ($p = 0.267$).

316 At station 3, many foraminifera were fragile under manipulation, and DS-5 specimens
317 were abundant through depth with about 140 ind.50cm⁻² (**Appendix**). At the SWI (0-2 mm
318 layer) and in the subsurface level (6-8-mm depth), DS-0 and DS-1 specimens represented
319 about 75 % while DS-2 accounted for 20 %. Few specimens of DS-3, DS-4 and DS-5 were
320 observed. At the deepest layer (40-50 mm), DS-5 specimens were the most abundant
321 calcareous tests foraminifera (78 %). The severe DS (DS-3, 4 and 5) were significantly
322 overrepresented in the deep layer than in the surface and subsurface layers ($p < 0.005$). DS
323 were not significantly different between surface and subsurface ($p = 1$).

324 Overall, the exact Fisher's test revealed significant difference dissolution stages among
325 stations ($p < 0.005$). The pair-wise Fisher's exact test showed that the low DS (0,1,2) were
326 significantly overrepresented at station 1 compared to the two other stations ($p < 0.005$).
327 Furthermore, there were no significant difference between stations 2 and 3 ($p = 0.532$).

328 **3.2.4 Calcareous vs. Agglutinated Foraminifera in the Dead Assemblages**

329 Species in the benthic foraminiferal thanatocoenosis were the same as in the living
330 assemblages. At station 1, calcareous taxa dominated agglutinated ones in the dead
331 assemblage with C/T ratio varying from 0.74 to 0.89 (**Table 3**). The proportion of organic lining
332 (DS-5/C) increased slightly with depth, from 0.06 to 0.18. On the other hand, at station 2,
333 agglutinated taxa dominated the dead assemblage in the surface and subsurface levels (C/T
334 ratio of 0.43 and 0.36 respectively) but not in the deepest one even if they remained abundant
335 (0.65; **Table 3**). The DS-5/C ratio was very high in all three depth layers, remaining > 0.70 . At
336 station 3, C/T ratio remained high in the dead assemblage of both surface and subsurface with
337 0.88, 0.83, and decreased strongly to 0.36 in depth where agglutinated specimens were
338 dominant. The DS-5/C ratio increased with depth, from 0.06 at the surface to 0.95 in the deeper
339 layer.

340 Comparing dead and living assemblages, it can be noted that for station 1, C/T ratio
341 were not very different whatever the depth (**Table 3**). Stations 2 and 3 showed much lower C/T
342 ratios in the dead assemblages indicating a marked loss of calcareous foraminifera during
343 taphonomic processes although this difference is not significant. In addition, stations 2 and 3

344 showed a higher occurrence of DS-5 tests in the dead assemblages resulting in high DS-5/C
 345 ratios. In detail, station 2 showed the highest DS-5/C ratio in the subsurface layer (0.96) where
 346 pH is minimal, while station 3 showed a strong increase of this ratio in the deepest layer (0.95).

347 **Table 3. Densities of living and dead foraminifera for each depth layer at the three all stations (ind.10 cm⁻³**
 348 **of sediment). Depth correspondences: surface (0-2 mm), subsurface (6-8 mm) and deep (4-5 mm). "Calcareous"**
 349 **class includes the DS-5 specimens (fully dissolved test showing the organic lining). A = agglutinated, C =**
 350 **calcareous, ratios are those described in the methods.**

		Living foraminifera					Dead foraminifera				
		Agglutinated (A)	Calcareous (C)	Fully dissolved test (DS-5)	C/T ratio	DS-5/C ratio	Agglutinated (A)	Calcareous (C)	Fully dissolved test (DS-5)	C/T ratio	DS-5/C ratio
St 1	surface [0-2 mm]	30	295	0	0.91	0.00	212	589	38	0.74	0.06
	subsurface [6-8 mm]	3	36	0	0.92	0.00	21	153	22	0.88	0.14
	deep [40-50 mm]	6	26	0	0.81	0.00	94	772	141	0.89	0.18
St 2	surface [0-2 mm]	4	137	1	0.97	0.01	373	282	197	0.43	0.70
	subsurface [6-8 mm]	7	12	2	0.63	0.17	181	104	100	0.36	0.96
	deep [40-50 mm]	1	4	2	0.80	0.50	239	453	327	0.65	0.72
St 3	surface [0-2 mm]	12	371	0	0.97	0.00	58	418	49	0.88	0.12
	subsurface [6-8 mm]	7	137	3	0.95	0.02	45	214	53	0.83	0.25
	deep [40-50 mm]	9	14	11	0.61	0.79	493	274	259	0.36	0.95

351 4 DISCUSSION

352 4.1 Is Cable Bacteria Density and Activity Responsible for 353 Porewater Acidification in the Mudflats of the Auray Estuary?

354 Oxygen and pH microprofiles recorded at stations 2 and 3 showed the typical fingerprint of
 355 CBA cable bacteria activity (CBA): a pH maximum within the oxic zone without oxygen
 356 production followed by a significant acidification into the suboxic zone (**Figure 4**; Nielsen et
 357 al., 2010; Pfeffer et al., 2012; Risgaard-Petersen et al., 2012; Meysman et al., 2015). The
 358 presence of CB cable bacteria within the upper first centimetre at station 2 was further
 359 confirmed by the qPCR data. ~~At station 2, the 16S CB copy number was constant within the~~
 360 ~~oxic and suboxic zones (upper first centimetre; Figure 4).~~ The calculated filament density of
 361 about 70 m.cm⁻³ at this station was in the same order of magnitude than the *in situ* densities
 362 reported from the Baltic sea (Marzocchi et al., 2018; Hermans et al., 2019), from bivalve reefs
 363 (Malkin et al., 2017), subtidal mudflats (van de Velde et al., 2016) or intertidal salt marshes
 364 (Larsen et al., 2015). The geochemical signature at station 1 is less clear regarding Cable
 365 Bacteria Activity (CBA) although ~~the qPCR data indicated very low CB filament density about~~
 366 ~~7 m.cm⁻³. The filament density was in the low range of the in situ densities reported from the~~
 367 ~~Baltic sea (Marzocchi et al., 2018; Hermans et al., 2019).~~ Here, ~~there~~ was no pH peak in the

368 oxic zone and the suboxic acidification was the weakest compared to stations 2 and 3 ($\Delta\text{pH} <$
369 1.0 and ΔpH of 2.3 and 1.6 respectively) only a moderate acidification within the suboxic zone
370 ($\Delta\text{pH} < 0.1$). As the sediment acidification continued at least 5 mm below the oxic zone (oxygen
371 penetration depth < 2 -mm depth) for the three stations, oxic processes such as pyrite oxidation
372 are unlikely to explain such pH decrease. However, the anaerobic oxidation of reduced
373 compounds such as manganese, iron or sulphide, could be involved in the porewater
374 acidification (Soetaert et al., 2007; Middelburg et al., 2020), but the observed acidification was
375 too high to be explained by such processes (van Cappellen and Wang, 1996; Soetaert et al.,
376 2007). Therefore, we suggested that acidification was mainly driven by cable bacteria activity
377 rather than any other geochemical process. This acidification was lower than expected if only
378 driven by sulphate reduction and too high to be explained by iron reduction (van Cappellen
379 and Wang, 1996; Soetaert et al., 2007). Therefore, we suggested that it was driven by low
380 CBA. The qPCR data indicated very low CB filament density about 7 m.cm^{-3} . The filament
381 density was in the low range of the *in situ* densities reported from the Baltic sea (Marzocchi et
382 al., 2018; Hermans et al., 2019).

383 The diversity of pH microprofiles observed between the three stations could indicate a
384 contrasted intensity of the CBA cable bacteria activity between stations. According to the low
385 filament abundance and the low range of pH ($\Delta\text{pH} = 1.0$) at station 1, ~~te~~ CBA would be minimal
386 and it would have limited impact on the sediment geochemistry. Conversely, the strong
387 abundance and pH range ($\Delta\text{pH} = 2.4$) suggest the most intense CBA cable bacteria activity at
388 station 2, whereas pH range ($\Delta\text{pH} = 1.8$) at station 3 suggests an intermediate to high CBA.

389 ~~Currently, the control factors of spatial and temporal variability of the CB density and~~
390 ~~the CBA on mudflats are still unresolved. It is possible that such variability from a mudflat to~~
391 ~~another can be explained by the stage of development of the bacterial community and/or by~~
392 ~~the specific geochemical composition of each mudflat from upstream to downstream (Malkin~~
393 ~~et al., 2014, 2017; Rao et al., 2016).~~ Our observations suggest that *Ulvae* mats observed at
394 stations 2 and 3 during core sampling in autumn (Table 1) could play a role on CB
395 development. Several studies showed that macrophyte decay is rather slow compared to
396 microphytobenthic mineralization and favours free-sulphide production and upward diffusion
397 (Anschutz et al., 2007; Metzger et al., 2007; Cesbron et al., 2014; Delgard et al., 2016) which
398 are favourable conditions to CB development. Previous observations confirm the rather high
399 spatial and temporal CBA seasonal cable bacteria activity dynamics ~~already mentioned in the~~
400 ~~literature~~ (e.g. Seitaj et al., 2015; Lipsewers et al., 2017; Hermans et al., 2019; Malkin et al.,
401 2022). Most publications refer to a boom-and-bust cycle of CB in laboratory incubations, and
402 to the seasonal alternation of the sulphur-oxidising bacterial community in the field as a

403 function of hypoxia events inducing seasonal pH variability. However, no desoxygenation or
404 strong and recursive reworking events have been reported in the present studied area during
405 the previous weeks before sampling, which is reoxygenated at each low tide (Fouet, 2022;
406 OFB and IFREMER data). Each low tide could lead to the reactivation of cable bacteria activity
407 in these highly eutrophic mudflats. The most intense resuspension phenomenon here would
408 be rising tide (Menier and Dubois, 2011; Menier et al., 2011) and bioturbation. The benthic
409 macrofauna (> 2 mm) of the mudflats is dominated by polychaetes *Nephtys* spp. known to
410 burrow into the sediments (Michaud et al., 2021); abundance around 8 ind.50cm⁻², pers. comm.
411 Oihana Latchere). The variability between the stations could be the result of bioturbation
412 modulating acidification within subsurface sediment layer (Malkin et al., 2014, 2017, 2022; Aller
413 et al., 2019). Unfortunately, there is little literature on cable bacteria activity under tidal cycle.
414 Currently, the control factors of spatial and temporal discrepancies of the cable bacteria density
415 and the CBA are still unresolved and need more investigations.

416 The cable bacteria activity causes pH anomalies that impact sediment geochemistry
417 and lead to the carbonate dissolution process as described in Risgaard-Petersen et al. (2012),
418 Meysman et al. (2015), Rao et al. (2016), van de Velde et al. (2016) and Malkin et al. (2017).
419 It has been supposed that this dissolution process could be responsible for foraminiferal test
420 dissolution (Risgaard-Petersen et al., 2012; Richirt et al., 2022). Considering the increase of
421 observations of cable bacteria activity occurrence in a wide range of coastal and marine
422 environments (Burdorf et al., 2017; Scholz et al., 2021), we assume that the potential impact
423 of this bacterial acidification of sediment on carbonate meiofauna should be strongly
424 considered.

425 **4.2 Impacts of Cable Bacteria Sediment Acidification on Living** 426 **Foraminifera**

427 ~~The CBA causes pH anomalies that impact sediment geochemistry and lead to the carbonate~~
428 ~~dissolution process as described in Risgaard-Petersen et al. (2012), Meysmann et al. (2015),~~
429 ~~van der Velde et al. (2016) and Rao et al. (2016). By analogy, it has been supposed that CBA~~
430 ~~could also be responsible for foraminifera dissolution (Risgaard-Petersen et al., 2012; Richirt~~
431 ~~et al., 2022). We showed in **Figure 4** and **Figure 6** that advanced dissolution stages 3, 4 and~~
432 ~~5 were significantly overrepresented at stations 2 and 3, where acidification was important,~~
433 ~~compared to station 1 where no DS-5 was observed. More precisely, vertical DS distribution~~
434 ~~corresponded to vertical acidity variability at stations 2 (0.01 < DS-5/C < 0.50) and 3 (0.00 <~~
435 ~~DS-5/C < 0.79). There iswas no indication for such depth distribution at station 1 where pH~~
436 ~~variability was the lowest (DS-5/C = 0). The relative abundance of calcareous specimens over~~
437 ~~agglutinated (C/T) iswas very stable along depth at station 1 (0.78 ± 0.07; **Appendix**) whereas~~

438 this ratio ~~is~~was more variable at stations 2 and 3 (0.65 ± 0.17 and 0.73 ± 0.15 respectively),
439 confirming that pH conditions affected ~~the~~ assemblage composition through the under
440 representation of calcareous foraminifera ~~although species diversity is never affected~~ (Figure
441 5). ~~Species diversity appeared to not be affected because most of the foraminiferal population~~
442 ~~lived in the thin oxic zone, which is not affected by the strong pH decrease. Assuming that~~
443 ~~acidification intensity in the suboxic zone is due to cable bacteria activity,~~ Our data suggest
444 that ~~CB~~ ~~the sediment acidification on the mudflats, supposedly due to cable bacteria activity,~~
445 ~~has~~have a drastic effect on the integrity of ~~shells~~from-living benthic foraminiferal ~~test~~ and
446 potentially on their assemblages. The magnitude of this effect may depend in the ~~CBA~~
447 ~~dissolution process~~ intensity and duration throughout the life cycle of foraminifera.-

448 Since the dataset of the present study is rather limited, one can examine literature data
449 that provides together oxygen and pH microprofiles with sub-centimetre vertical distribution of
450 living foraminifera in intertidal mudflats first and other benthic environments ~~then~~. Geochemical
451 data from an intertidal mudflat of the Arcachon basin in the French Atlantic coast suggest ~~CBA~~
452 ~~sediment acidification~~ in May 2011 at ~~N~~-station ~~N~~ (Cesbron et al., 2016) with a $\Delta\text{pH} = 1.6$ and
453 a pH minimum of 6.2 well below the oxic zone at 20-mm depth. At the same station in July
454 2011, all calcareous benthic foraminifera specimens showed a fully dissolved test with the
455 organic lining remaining ($\text{DS-5/C} = 1$). The assemblage also showed that, *Eggerella scabra*,
456 an agglutinated species, strongly dominated the foraminiferal assemblage at all depths down
457 to 50 mm, except for the 0 to 5 mm layer ($\text{C/T} = 0.88 \pm 0.02$ for the uppermost layer; $\text{C/T} = 0$
458 below). The authors assumed that test dissolution resulted from a strong acidification of the
459 sediments due to an intense remineralisation of the relict roots of *Zostera*. We can assume
460 here that these roots provided the refractory material that enhanced sulphate reduction
461 (Anschutz et al., 2007; Metzger et al., 2007; Cesbron et al., 2014; Delgard et al., 2016),
462 providing enough free-sulphide to favour ~~CB~~ ~~cable bacteria~~ development that ~~drove~~ ~~could drive~~
463 the dissolution process as it probably happened at stations 2 and 3 of the Auray estuary in the
464 present study. However, Cesbron and co-workers also showed that during winter (February
465 2011), foraminifera showed less dissolution due to a lower intensity of diagenetic processes
466 including free-sulphide production and probably benthic acidification. These results underline
467 the importance of the temporal variability of diagenetic processes that influence pore water
468 geochemistry ~~including CBA (Seitaj et al., 2015; Lipsewers et al., 2017; Hermans et al., 2019;~~
469 ~~Malkin et al., 2022),~~ and eventually calcareous test integrity. It also questions about time
470 integration of pH conditions recorded in the foraminifera tests as foraminifera may have
471 mechanisms to buffer pH variations as suggested by different studies (de Nooijer et al., 2009b,
472 2014; Toyofuku et al., 2017) or vertical migration strategies (Geslin et al., 2004; Pucci et al.,
473 2009; Koho et al., 2011; Hess et al., 2013). It could be assumed that the dissolution of the

474 calcareous foraminifera tests would respond to ~~an~~-integrated dynamics over a few days to a
475 few weeks (Le Cadre, 2003; Charrieau et al., 2018b, 2022); Daviray, pers. com.). These
476 microorganisms are capable of recalcifying their test following acidification events with the
477 same daily to weekly dynamics (Le Cadre et al., 2003). This dynamic is relatively comparable
478 to the oxidation processes of the reduced mineral phases that can generate acidification of the
479 sediment as is cable bacteria activity. We therefore assume that the tests of dead specimens
480 incorporate the variability of these dynamics to a greater or lesser extent~~several months of~~
481 ~~exposure to the acidity caused by CBA, rather than immediately~~. These dynamics should be
482 investigated in the future in Auray estuary to better understand differences of dissolution
483 stages observed between stations. It can also be assumed that tolerance to acidification may
484 be species-dependent ~~and needs detailed investigation~~. Under laboratory experiments,
485 Charrieau et al. (2018) have shown that *Ammonia* sp. specimens survived longer than
486 *Elphidium crispum* under the same conditions of salinity, pH and Ω_{calc} (20-34, 7.3-7.9 and 0.4-
487 2.7 respectively). ~~(Mojtahid et al., (2023) have observed that low DIC ($< 900 \mu\text{mol.kg}^{-1}$) affected~~
488 growth and survival of *Bulimina marginata* and *Cassidulina laevigata* but not *Ammonia*
489 *confestitesta*, while a pH and Ω_{calc} decrease did not affect any of the three species (other
490 parameters constant, $\text{pH} > 7.5$, $\Omega_{\text{calc}} \geq 1$). ~~(McIntyre-Wressnig et al., (2014) have seen no effect~~
491 of acidification on *Bolivina argentea* and *Bulimina marginata* (S~34, TA~2400 $\mu\text{mol.kg}^{-1}$, $\text{pH} \geq$
492 7.5). Furthermore, ~~(Haynert et al., (2011) have shown that *Ammonia aomoriensis* slightly~~
493 decalcified as soon as $\text{pH} \sim 7.7$ and $\Omega_{\text{calc}} > 1$, and showed severe dissolution at $\text{pH} \leq 7.4$ and
494 $\Omega_{\text{calc}} < 1$. However, the same species cultured in their natural sediment was unaffected in the
495 same geochemical conditions (Haynert et al., 2014). It suggests that sediment chemistry
496 provides a microhabitat to support benthic foraminiferal community growth and development
497 even under sediment acidification. These interesting results have emphasized the complex
498 and misunderstood interaction between calcareous test foraminifera and the carbonate system
499 that need more detailed investigations.

500 Conversely, a tidal mudflat from another estuarine system of French Atlantic coast
501 seems not to show indices of ~~CBA~~-acidification process nor occurrence of dissolution on living
502 foraminifera. Living foraminifera from the Brillantes mudflat of Loire estuary was studied at two
503 stations in September 2012 and April 2013 (Thibault de Chanvalon et al., 2015, 2022). The
504 vertical distribution of living foraminifera reported in the Loire mudflat was similar to the vertical
505 distribution of station 2 reported in the present study with a maximal density at the topmost
506 layer within the oxic zone, a minimal density around 10-mm depth and a second maximum
507 below. However, no foraminiferal test dissolution was reported by Thibault de Chanvalon and
508 co-workers and the foraminiferal assemblages were heavily dominated by calcareous
509 foraminiferal species, resulting in a DS-5/C ratio equal to zero and a C/T ratio about 1.

510 Furthermore, at these stations, pH profiles did not show strong acidification or signs of CBA
511 fingerprint at different occasions (May 2013, February 2014, June 2018, unpublished data).
512 pH decrease corresponded to oxygen uptake and was below 0.5 units with a minimum about
513 7.7. No pH peak at the interface was observed in a profile performed in the dark neither. The
514 major difference between these systems is the size of the river that induces significant
515 resuspension-deposition events for the Loire estuary (network SYVEL. GIP Loire Estuaire)
516 limiting the development of favourable conditions to CB development. In addition, bioturbation
517 seems to be intense at the Brillantes mudflat (Thibault de Chanvalon et al., 2015, 2016b, 2017).
518 Another difference between these studies is the absence of macrophytes at the studied
519 stations of the Brillantes mudflat. Finally the size of the catchment area of Loire provides an
520 important flux of suspended particles rich in metallic oxides that will once settled in the mudflat
521 generate a thick layer of sediment where the iron cycle dominates diagenetic processes acting
522 as an efficient “iron curtain” that maintains free-sulphide between 5 to 10 cm depth (Thibault
523 de Chanvalon et al., 2016a, b) to be out of reach for CB. These combined conditions are not
524 favourable to CB-cable bacteria development (Malkin et al., 2014, 2017). This, foraminiferal
525 observations strongly suggest the absence of CBA-dissolution process in the studied part of
526 the Brillantes mudflat. This area may be considered as a control station.

527 Other studies reporting calcareous test dissolution of benthic living foraminifera in
528 comparable transitional environments are published but without geochemical data, allowing to
529 discuss potential causes of the dissolution process CBA (Alve and Nagy, 1986; Buzas-
530 Stephens, 2005; Polovodova and Schonfeld, 2008; Bentov et al., 2009; de Nooijer et al., 2009;
531 Kurtarkar et al., 2011; Haynert et al., 2012; Schönfeld and Mendes, 2022). Although the
532 hypotheses put forward by these authors on the causes of test dissolution are all plausible
533 (environmental pollution, freshwater inputs, organic matter degradation), they are not strongly
534 explained. Therefore, the absence of pH data (Buzas-Stephens, 2005; Polovodova and
535 Schonfeld, 2008) or its insufficient vertical resolution (Alve and Nagy, 1986; Haynert et al.,
536 2012; Schönfeld and Mendes, 2022) do not exclude the potential involvement of CB-cable
537 bacteria in those environments. In the Baltic sea, that could be considered as a sort of giant
538 estuary, Charrieau et al. (2018a), provide pH microprofiles that seem to indicate the absence
539 of CBA strong acidification (all sites combined: minimum pH = 7.17; maximum ΔpH = 0.6).
540 However, these authors observed calcareous test dissolution of living foraminifera and
541 concluded that dissolution may be the consequence of a complex set of environmental factors
542 whose ecological equilibrium can change rapidly in such coastal areas (salinity, oxygen
543 concentration, pH and Ω_{calc}). Laboratory experiments conducted by these authors (Charrieau
544 et al., 2018b), seem to indicate that low salinity may be an important factor on calcareous test
545 dissolution. The difference with estuarine studies discussed above is probably that salinity

546 change dynamics in the Baltic is rather minor compared to salinity in Auray and Loire that are
547 macrotidal systems with species adapted to such salinity variations.

548 ~~Considering the increase of observations of cable bacteria activity occurrence in a wide~~
549 ~~range of marine environments (Malkin et al., 2014; Burdorf et al., 2017) like estuaries, coastal~~
550 ~~lagoons, salt marshes, marine lakes, tidal and subtidal mudflats, we assume that the impact~~
551 ~~of CBA on foraminifera community should be strongly considered.~~

552 **4.3 Impacts of Cable Bacteria Sediment Acidification on Dead** 553 **Assemblages and Shell Preservation**

554 Richirt et al. (2022) have assumed that calcium carbonate undersaturation in suboxic zone
555 ~~calcareous test dissolution~~ resulting from CBA cable bacteria activity could be responsible for
556 low densities of calcareous tests in the dead assemblages recorded in sediments of Lake
557 Grevelingen. Our results suggest that acidification, as caused by CBA could induce, strongly
558 affects the calcareous ~~shell test~~ integrity and the assemblage composition of living foraminifera
559 before taphonomic processes. Our study also suggests that after foraminifera death, CBA
560 dissolution processes keeps transforming the foraminifera assemblage during test burial
561 ~~confirming supporting~~ the hypothesis formulated by Richirt and coworkers (2022). Comparing
562 C/T and DS-5/C ratios between living and dead assemblages at different depths we relate in
563 detail the impact of pH distribution ~~and therefore CBA~~ to the taphonomic loss. Under a weak
564 CBA low acidification (like at station 1), calcareous tests were relatively well preserved. At this
565 station, the community structure between living and dead assemblages varied slightly (C/T
566 ranged from 0.81- to 0.98 in living assemblage and from 0.74- to 0.89 in dead assemblage).
567 The occurrence of dissolution in the living assemblage was nil while in the dead assemblage
568 the DS-5/C ratio increased with depth from 0.06 to 0.18 indicating that the low dissolution
569 generated a relatively slow taphonomic process. Calcareous tests dominated both living and
570 dead assemblages with an increase of this trend with depth in the dead assemblage confirming
571 the good preservation of calcareous foraminifera. Where CBA sediment acidification was
572 moderate (like at station 3), the dissolution effect on the thanatocoenosis was gradual with
573 depth. Calcareous test density decreased through the wide acidic layer (C/T decrease from
574 above 0.8 to 0.36 at 50-mm depth) and there was an accumulation of fully dissolved tests
575 showing only their organic linings in dead foraminiferal assemblages at depth (DS-5/C of 0.95).
576 This feature suggests that the moderate dissolution generated a gradual taphonomic process
577 leading to a noticeable calcareous loss with depth. Eventually, under a strong and intense CBA
578 dissolution process (like at station 2), the ~~dissolution~~ effect occurred mostly within the restricted
579 acidic layer. The calcareous tests disappeared from the dead foraminiferal assemblage in this
580 subsurface layer while the fully dissolved tests showing only their organic linings and

581 agglutinated tests accumulated ($C/T = 0.37$ and $DS-5/C = 0.96$). At depth, the dead
582 foraminiferal assemblage showed fairly high densities that are comparable to stations where
583 ~~CBA acidification~~ was less intense. As the living specimens were quite rare, such accumulation
584 of dead tests suggested that somehow they bypassed the acidic firewall of the suboxic layer.
585 If tests arrived at depth through sedimentary burial the acidic firewall was possibly variable
586 through time and not active in a recent past constantly established. If ~~CBA sediment~~
587 ~~acidification~~ is ~~not recent~~ more constant, physical or biological reworking buried sufficiently fast
588 to preserve tests from corrosive conditions and mechanic crumbling. Here, regardless of the
589 alkalinity or calcium carbonate content of the sediment, if living and dead calcareous
590 foraminifera are decalcified so intensely, the corrosive conditions are intense enough over time
591 to generate dissolution in organisms, which alive can fight off these hostile conditions to a
592 greater or lesser extent, as they are somehow adapted to the strong physical and
593 biogeochemical dynamics of transitional environments.

594 At this stage, these hypotheses cannot be assessed. One can note the high concentration of
595 dead fully dissolved tests in the first 2 mm (0.70) where pH is the most alkaline suggesting that
596 sedimentary reworking may have brought dead specimens from the subsurface acidic layer to
597 the surface. Further studies on dead assemblages are needed to statistically validate the CBA
598 vs. calcareous test loss relationship.

599 With low pH and carbonate undersaturation in pore water, the dissolution process
600 resulting from ~~CBA cable bacteria activity suggests and could leave an~~ imprint on taphonomy
601 and on historical records yet to be explored. Indeed, it may alter the carbonate composition of
602 the remaining calcareous tests used to geochemical proxies based on isotopic fractioning or
603 trace elements (Katz et al., 2010; Petersen et al., 2018; Mojtahid et al., 2023).

604 In this case, Dissolution of living and dead calcareous test foraminifera due to CBA may
605 be ~~taken into account~~ considered as a potential factor in the seasonal perturbation of sediment
606 geochemistry in interpretations of foraminiferal assemblages ~~in~~ of historical studies. As
607 proposed in Richirt et al. (2022), historical records of benthic foraminifera could ~~also~~ be used
608 to reconstruct past CBA and determine the age of the first ~~CB cable bacteria~~ occurrence in the
609 studied environments. A multivariate approach coupling the identification of lipid biomarkers in
610 cable bacteria or eDNA, the study of foraminiferal species assemblages (C/T ratio), test
611 preservation and isotopic test composition and the characterisation of the paleoenvironment
612 by sedimentology and sediment geochemistry could allow us to distinguish the bacterial activity
613 from other factors responsible for test dissolution. Therefore, associating it with major
614 environmental changes through time, light could be shed on the original factors of this bacterial
615 spreading discovered only ten years ago: have they always been present without us having

616 the tools to detect them, or have they appeared recently and are they spreading around the
617 world?

618 **5 CONCLUSION**

619 This original study ~~strongly~~ suggests that sediment acidification caused by CBA-cable bacteria
620 activity could be responsible for significant calcareous test foraminifera dissolution patterns.
621 As a result, proportions of calcareous test would change in both living and dead assemblages.
622 The proportion of fully dissolved tests showing only their organic linings would increase in the
623 living assemblages in the suboxic and anoxic zones of the sediment, as well as in the
624 thanatocoenosis. In order to better understand this cause-and-effect relationship and reduce
625 the uncertainty factors raised here, further *in situ* studies would need to be carried out in further
626 locations over different periods, especially including the carbonate system. Laboratory
627 incubation experiments would provide also a better understanding~~The spatial dynamics of~~
628 ~~calcareous test dissolution in mudflats described in the present study seems to be the~~
629 ~~consequence of CBA which leads to a wide range of pore water pH in the suboxic zone of~~
630 ~~sediment.~~

631 ~~Now that we have an idea_~~ of the potential impact of this bacterial activity on the resilience of
632 foraminiferal communities. It should allow us to learn more about the integration of their
633 response in the historic record~~on foraminiferal assemblages and on calcareous test~~
634 ~~preservation~~ Based on these hypotheses, we are entitled to ask what implications ~~this~~ they
635 might have for environmental interpretations of data from ~~their~~ foraminifera use as
636 paleoproxies, or bioindicators. ~~In order to better understand this impact, it would be relevant to~~
637 ~~explore *in situ* and *in vitro* the effect of CBA at several time scales on the resilience of~~
638 ~~foraminiferal communities to learn more about the integration of their response in the~~
639 ~~historic/fossil record.~~ Eventually, we ~~shc~~ could be able to provide a historical retrospective on
640 the presence of CB-cable bacteria in marine sediments and their impact on the carbonate
641 system and benthic meiofauna. ~~In this perspective, we should combine such studies with the~~
642 ~~development of biomarkers of these chemolithoautotrophic bacteria or of ancient eDNA.~~

643 *Data availability.* All of the data are published within this paper and in the Supplement. The
644 raw data used to make the figures are available on request.

645 *Author contributions.* Maxime DAVIRAY (foraminiferal and geochemical analysis, writing,
646 review and editing), Emmanuelle GESLIN (head of CB-For CNRS project, foraminiferal
647 analysis, writing, review and editing), Nils RISGAARD-PETERSEN (statistical inference, writing,
648 review and editing), Vincent SCHOLZ (qPCR proceeding, review and editing), Marie FOUET
649 (field work, review and editing), Edouard METZGER (microprofile acquisition, writing, review and
650 editing).

651 *Competing interests.* At least one of the (co-)authors is a member of the editorial board of
652 Biogeosciences.

653 *Acknowledgments.* The authors are grateful to Sophie QUINCHARD for assistance with the
654 foraminifera picking, Sophie SANCHEZ for sample splitting (LPG, Université d'Angers) and
655 Romain MALLET (SCIAM, Université d'Angers) for the achievement of a part of the SEM
656 imaging. Susanne NIELSEN and Ian MARSHALL (Aarhus University) are thanked for assistance
657 with the qPCR analysis. The authors are grateful to Frans JORISSEN for field work, and his
658 advice for the writing process (LPG, Université d'Angers). The authors thank the participants
659 to the field trips (2019 and 2020). The authors also thank Sebastiaan van de Velde and the
660 two anonymous reviewers for their constructive comments.

661 *Financial support.* The authors received funding from the CNRS-INSU (program LEFE-
662 CYBER, project CB-FOR), from the Angers University and from the OFB (project FORESTAT).

663 REFERENCES

664 Aller, R. C., Aller, J. Y., Zhu, Q., Heilbrun, C., Klingensmith, I., and Kaushik, A.: Worm tubes
665 as conduits for the electrogenic microbial grid in marine sediments, *Science Advances*, 5,
666 eaaw3651, <https://doi.org/10.1126/sciadv.aaw3651>, 2019.

667 Alve, E., and Nagy, J. (1986). Estuarine foraminiferal distribution in Sandebukta, a branch of
668 the Oslo Fjord (Norway). *Journal of Foraminiferal Research - J FORAMIN RES* 16, 261–284.
669 doi: 10.2113/gsjfr.16.4.261.

670 Anschutz, P., Chaillou, G., and Lecroart, P. (2007). Phosphorus diagenesis in sediment of the
671 Thau Lagoon. *Estuarine, Coastal and Shelf Science* 72, 447–456. doi:
672 10.1016/j.ecss.2006.11.012.

673 Balsamo, M., Semprucci, F., Frontalini, F., and Coccioni, R. (2012). “Meiofauna as a Tool for
674 Marine Ecosystem Biomonitoring,” in *Marine ecosystems* (InTech), 77–104.

675 Bentov, S., Brownlee, C., and Erez, J. (2009). The role of seawater endocytosis in the
676 biomineralization process in calcareous foraminifera. *Proceedings of the National Academy of*
677 *Sciences* 106, 21500–21504. doi: 10.1073/pnas.0906636106.

678 Bernhard, J. M., and Bowser, S. S. (1996). Novel epifluorescence microscopy method to
679 determine life position of foraminifera in sediments. *J. Micropalaeontol.* 15, 68–68. doi:
680 10.1144/jm.15.1.68.

681 Bernhard, J. M., Ostermann, D. R., Williams, D. S., and Blanks, J. K. (2006). Comparison of
682 two methods to identify live benthic foraminifera: A test between Rose Bengal and CellTracker
683 Green with implications for stable isotope paleoreconstructions: Foraminifera Viability Method
684 Comparison. *Paleoceanography* 21. doi: 10.1029/2006PA001290.

685 Boudagher-Fadel, M. K. (2018). “Biology and Evolutionary History of Larger Benthic
686 Foraminifera,” in *Evolution and Geological Significance of Larger Benthic Foraminifera* (UCL
687 Press), 1–44. doi: 10.2307/j.ctvqhsq3.3.

688 Burdorf, L. D. W., Trammer, A., Seitaj, D., Meire, L., Hidalgo-Martinez, S., Zetsche, E.-M., et
689 al. (2017). Long-distance electron transport occurs globally in marine sediments.
690 *Biogeosciences* 14, 683–701. doi: 10.5194/bg-14-683-2017.

691 Buzas-Stephens, P. (2005). Population Dynamics and Dissolution of Foraminifera in Nueces
692 Bay, Texas. *The Journal of Foraminiferal Research* 35, 248–258. doi: 10.2113/35.3.248.

- 693 Cesbron, F., Metzger, E., Launeau, P., Deflandre, B., Delgard, M.-L., Thibault de Chanvalon,
694 A., et al. (2014). Simultaneous 2D Imaging of Dissolved Iron and Reactive Phosphorus in
695 Sediment Porewaters by Thin-Film and Hyperspectral Methods. *Environ. Sci. Technol.* 48,
696 2816–2826. doi: 10.1021/es404724r.
- 697 Cesbron, F., Geslin, E., Jorissen, F. J., Delgard, M. L., Charrieau, L., Deflandre, B., et al.
698 (2016). Vertical distribution and respiration rates of benthic foraminifera: Contribution to
699 aerobic remineralization in intertidal mudflats covered by *Zostera noltei* meadows. *Estuarine,
700 Coastal and Shelf Science* 179, 23–38. doi: 10.1016/j.ecss.2015.12.005.
- 701 Charrieau, L. M., Bryngemark, L., Hansson, I., and Filipsson, H. L. (2018a). Improved wet
702 splitter for micropalaeontological analysis, and assessment of uncertainty using data from
703 splitters. *J. Micropalaeontol.* 37, 191–194. doi: 10.5194/jm-37-191-2018.
- 704 Charrieau, L. M., Filipsson, H. L., Ljung, K., Chierici, M., Knudsen, K. L., and Kritzberg, E.
705 (2018b). The effects of multiple stressors on the distribution of coastal benthic foraminifera: A
706 case study from the Skagerrak-Baltic Sea region. *Marine Micropaleontology* 139, 42–56. doi:
707 10.1016/j.marmicro.2017.11.004.
- 708 Charrieau, L. M., Filipsson, H. L., Nagai, Y., Kawada, S., Ljung, K., Kritzberg, E., et al. (2018c).
709 Decalcification and survival of benthic foraminifera under the combined impacts of varying pH
710 and salinity. *Marine Environmental Research* 138, 36–45. doi:
711 10.1016/j.marenvres.2018.03.015.
- 712 Charrieau, L. M., Nagai, Y., Kimoto, K., Dissard, D., Below, B., Fujita, K., and Toyofuku, T.:
713 The coral reef-dwelling *Peneroplis* spp. shows calcification recovery to ocean acidification
714 conditions, *Sci Rep*, 12, 6373, <https://doi.org/10.1038/s41598-022-10375-w>, 2022.
- 715 Choquel, C., Geslin, E., Metzger, E., Filipsson, H. L., Risgaard-Petersen, N., Launeau, P., et
716 al. (2021). Denitrification by benthic foraminifera and their contribution to N-loss from a fjord
717 environment. *Biogeosciences* 18, 327–341. doi: 10.5194/bg-18-327-2021.
- 718 Corliss, B. H., and Honjo, S. (1981). Dissolution of Deep-Sea Benthonic Foraminifera.
719 *Micropaleontology* 27, 356. doi: 10.2307/1485191.
- 720 de Nooijer, L. J., Toyofuku, T., and Kitazato, H. (2009). Foraminifera promote calcification by
721 elevating their intracellular pH. *Proceedings of the National Academy of Sciences* 106, 15374–
722 15378. doi: 10.1073/pnas.0904306106.
- 723 de Nooijer, L. J., Spero, H. J., Erez, J., Bijma, J., and Reichart, G. J. (2014). Biomineralization
724 in perforate foraminifera. *Earth-Science Reviews* 135, 48–58. doi:
725 10.1016/j.earscirev.2014.03.013.
- 726 Debenay, J.-P., Guillou, J.-J., Redois, F., and Geslin, E. (2000). “Distribution Trends of
727 Foraminiferal Assemblages in Paralic Environments,” in *Environmental Micropaleontology:
728 The Application of Microfossils to Environmental Geology Topics in Geobiology.*, ed. R. E.
729 Martin (Boston, MA: Springer US), 39–67. doi: 10.1007/978-1-4615-4167-7_3.
- 730 Debenay, J.-P., Bicchi, E., Goubert, E., and Armynot du Châtelet, E. (2006). Spatio-temporal
731 distribution of benthic foraminifera in relation to estuarine dynamics (Vie estuary, Vendée, W
732 France). *Estuarine, Coastal and Shelf Science* 67, 181–197. doi: 10.1016/j.ecss.2005.11.014.
- 733 Delgard, M. L., Deflandre, B., Kochoni, E., Avaro, J., Cesbron, F., Bichon, S., et al. (2016).
734 Biogeochemistry of dissolved inorganic carbon and nutrients in seagrass (*Zostera noltei*)
735 sediments at high and low biomass. *Estuarine, Coastal and Shelf Science* 179, 12–22. doi:
736 10.1016/j.ecss.2016.01.012.

- 737 Durand, M., Mojtahid, M., Maillet, G. M., Baltzer, A., Schmidt, S., Blet, S., et al. (2018). Late
738 Holocene record from a Loire River incised paleovalley (French inner continental shelf):
739 Insights into regional and global forcing factors. *Palaeogeography, Palaeoclimatology,*
740 *Palaeoecology* 511, 12–28. doi: 10.1016/j.palaeo.2018.06.035.
- 741 Envlit Bassin Loire-Bretagne. Available online: [https://wwz.ifremer.fr/envlit/DCE/La-DCE-par-](https://wwz.ifremer.fr/envlit/DCE/La-DCE-par-bassin/Bassin-Loire-Bretagne)
742 [bassin/Bassin-Loire-Bretagne](https://wwz.ifremer.fr/envlit/DCE/La-DCE-par-bassin/Bassin-Loire-Bretagne) (accessed on 29 Novembre 2023).
- 743 Fouet, M. P. A., Singer, D., Coynel, A., Héliot, S., Howa, H., Lalande, J., et al. (2022).
744 Foraminiferal Distribution in Two Estuarine Intertidal Mudflats of the French Atlantic Coast:
745 Testing the Marine Influence Index. *Water* 14, 645. doi: 10.3390/w14040645.
- 746 Fouet, M.: Répartition des communautés de foraminifères dans les estuaires de la façade
747 atlantique, Thèse de doctorat, Université d'Angers, Université d'Angers, 270 pp., 2022.
- 748 Geelhoed, J. S., van de Velde, S. J., and Meysman, F. J. R. (2020). Quantification of Cable
749 Bacteria in Marine Sediments via qPCR. *Frontiers in Microbiology* 11, 1506. doi:
750 10.3389/fmicb.2020.01506.
- 751 Geslin, E., Heinz, P., Jorissen, F., and Hemleben, Ch. (2004). Migratory responses of deep-
752 sea benthic foraminifera to variable oxygen conditions: laboratory investigations. *Marine*
753 *Micropaleontology* 53, 227–243. doi: 10.1016/j.marmicro.2004.05.010.
- 754 Gonzales, M. V., De Almeida, F. K., Costa, K. B., Santarosa, A. C. A., Camillo, E., De Quadros,
755 J. P., et al. (2017). Helpd Index: *Hoeglundina elegans* Preservation Index for Marine
756 Sediments in the Western South Atlantic. *Journal of Foraminiferal Research* 47, 56–69. doi:
757 10.2113/gsjfr.47.1.56.
- 758 Hansen, H. J. (1999). “Shell construction in modern calcareous Foraminifera,” in *Modern*
759 *Foraminifera* (Dordrecht: Springer Netherlands), 57–70. doi: 10.1007/0-306-48104-9_4.
- 760 Haynert, K., Schönfeld, J., Riebesell, U., and Polovodova, I. (2011). Biometry and dissolution
761 features of the benthic foraminifer *Ammonia aomoriensis* at high pCO₂. *Marine Ecology*
762 *Progress Series* 432, 53–67. doi: 10.3354/meps09138.
- 763 Haynert, K., Schönfeld, J., Polovodova-Asteman, I., and Thomsen, J. (2012). The benthic
764 foraminiferal community in a naturally CO₂-rich coastal habitat of the southwestern Baltic Sea.
765 *Biogeosciences* 9, 4421–4440. doi: 10.5194/bg-9-4421-2012.
- 766 Haynert, K., Schönfeld, J., Schiebel, R., Wilson, B., and Thomsen, J. (2014). Response of
767 benthic foraminifera to ocean acidification in their natural sediment environment: a long-term
768 culturing experiment. *Biogeosciences* 11, 1581–1597. doi: 10.5194/bg-11-1581-2014.
- 769 Haynes, J. R. (1981). *Foraminifera*. Springer.
- 770 Hermans, M., Lenstra, W. K., Hidalgo-Martinez, S., van Helmond, N. A. G. M., Witbaard, R.,
771 Meysman, F. J. R., et al. (2019). Abundance and Biogeochemical Impact of Cable Bacteria in
772 Baltic Sea Sediments. *Environ. Sci. Technol.* 53, 7494–7503. doi: 10.1021/acs.est.9b01665.
- 773 Hess, S., Alve, E., Trannum, H. C., and Norling, K. (2013). Benthic foraminiferal responses to
774 water-based drill cuttings and natural sediment burial: Results from a mesocosm experiment.
775 *Marine Micropaleontology* 101, 1–9. doi: 10.1016/j.marmicro.2013.03.004.
- 776 Jorissen, F. J., Fouet, M. P. A., Singer, D., and Howa, H. (2022). The Marine Influence Index
777 (MII): A Tool to Assess Estuarine Intertidal Mudflat Environments for the Purpose of
778 Foraminiferal Biomonitoring. *Water* 14, 676. doi: 10.3390/w14040676.

- 779 Jorissen, F. J., Fouet, M. P. A., Armynot du Châtelet, E., Barras, C., Bouchet, V. M. P., Daviray,
780 M., et al. (2023). *Foraminifères estuariens de la façade atlantique française - Guide de*
781 *détermination*. Université d'Angers; OFB.
- 782 Kassambara A (2022). *_rstatix: Pipe-Friendly Framework for Basic Statistical Tests_*. R
783 package version 0.7.1, <https://CRAN.R-project.org/package=rstatix>.
- 784 Katz, M. E., Cramer, B. S., Franzese, A., Hönisch, B., Miller, K. G., Rosenthal, Y., et al. (2010).
785 Traditional and Emerging Geochemical Proxies in Foraminifera. *Journal of Foraminiferal*
786 *Research* 40, 165–192. doi: 10.2113/gsjfr.40.2.165.
- 787 Keul, N., Langer, G., Thoms, S., de Nooijer, L. J., Reichart, G.-J., and Bijma, J. (2017).
788 Exploring foraminiferal Sr/Ca as a new carbonate system proxy. *Geochimica et Cosmochimica*
789 *Acta* 202, 374–386. doi: 10.1016/j.gca.2016.11.022.
- 790 Koho, K. A., Piña-Ochoa, E., Geslin, E., and Risgaard-Petersen, N. (2011). Vertical migration,
791 nitrate uptake and denitrification: survival mechanisms of foraminifers (*Globobulimina turgida*)
792 under low oxygen conditions: Survival mechanisms of foraminifers. *FEMS Microbiology*
793 *Ecology* 75, 273–283. doi: 10.1111/j.1574-6941.2010.01010.x.
- 794 Kurtarkar, S. R., Nigam, R., Saraswat, R., and Linshy, V. N. (2011). Regeneration and
795 Abnormality in Benthic Foraminifera *Rosalina leei*: Implications in Reconstructing Past Salinity
796 Changes. *Rivista Italiana Di Paleontologia e Stratigrafia*, 189-196.
- 797 Langlet, D., Geslin, E., Baal, C., Metzger, E., Lejzerowicz, F., Riedel, B., et al. (2013).
798 Foraminiferal survival after long-term *in situ* experimentally induced anoxia. *Biogeosciences*
799 10, 7463–7480. doi: 10.5194/bg-10-7463-2013.
- 800 Langlet, D., Baal, C., Geslin, E., Metzger, E., Zuschin, M., Riedel, B., et al. (2014).
801 Foraminiferal species responses to *in situ*, experimentally induced anoxia in the Adriatic Sea.
802 *Biogeosciences* 11, 1775–1797. doi: 10.5194/bg-11-1775-2014.
- 803 Le Cadre, V. (2003). Low pH Effects on *Ammonia beccarii* Test Deformation: Implications for
804 Using Test deformations as a Pollution Indicator. *The Journal of Foraminiferal Research* 33,
805 1–9. doi: 10.2113/0330001.
- 806 Lipsewers, Y. A., Vasquez-Cardenas, D., Seitaj, D., Schauer, R., Hidalgo-Martinez, S.,
807 Sinninghe Damsté, J. S., et al. (2017). Impact of Seasonal Hypoxia on Activity and Community
808 Structure of Chemolithoautotrophic Bacteria in a Coastal Sediment. *Appl Environ Microbiol* 83.
809 doi: 10.1128/AEM.03517-16.
- 810 Malkin, S. Y., Rao, A. M., Seitaj, D., Vasquez-Cardenas, D., Zetsche, E.-M., Hidalgo-Martinez,
811 S., et al. (2014). Natural occurrence of microbial sulphur oxidation by long-range electron
812 transport in the seafloor. *ISME J* 8, 1843–1854. doi: 10.1038/ismej.2014.41.
- 813 Malkin, S. Y., Seitaj, D., Burdorf, L. D. W., Nieuwhof, S., Hidalgo-Martinez, S., Tramper, A., et
814 al. (2017). Electrogenic Sulfur Oxidation by Cable Bacteria in Bivalve Reef Sediments. *Front.*
815 *Mar. Sci.* 4. doi: 10.3389/fmars.2017.00028.
- 816 Malkin, S. Y., Liao, P., Kim, C., Hantsoo, K. G., Gomes, M. L., and Song, B. (2022). Contrasting
817 controls on seasonal and spatial distribution of marine cable bacteria (*Candidatus Electrothrix*)
818 and *Beggiatoaceae* in seasonally hypoxic Chesapeake Bay. *Limnology and Oceanography* 67,
819 1357–1373. doi: 10.1002/lno.12087.

- 820 Martin, R. E. (2000). *Environmental Micropaleontology: The Application of Microfossils to*
821 *Environmental Geology*. Kluwer Academic/Plenum Publishers. Springer Available at:
822 <https://doi.org/10.1007/978-1-4615-4167-7>.
- 823 Marzocchi, U., Trojan, D., Larsen, S., Louise Meyer, R., Peter Revsbech, N., Schramm, A., et
824 al. (2014). Electric coupling between distant nitrate reduction and sulfide oxidation in marine
825 sediment. *ISME J* 8, 1682–1690. doi: 10.1038/ismej.2014.19.
- 826 McIntyre-Wressnig, A., Bernhard, J. M., Wit, J. C., and Mccorkle, D. C.: Ocean acidification
827 not likely to affect the survival and fitness of two temperate benthic foraminifera species: results
828 from culture experiments, *Journal of Foraminiferal Research*, 44, 341–351,
829 <https://doi.org/10.2113/gsjfr.44.4.341>, 2014.
- 830 Menier, D. and Dubois, A.: Carte 7137G Natures de fond du Golfe du Morbihan à 1/20 000,
831 Service Hydrographique & Océanographique de la Marine, (S.H.O.M), 2011.
- 832 Menier, D., Tessier, B., Dubois, A., Goubert, E., and Sedrati, M.: Geomorphological and
833 hydrodynamic forcing of sedimentary bedforms - Example of Gulf of Morbihan (South Brittany,
834 Bay of Biscay), *Journal of Coastal Research*, 1530–1534, 2011.
- 835 Metzger, E., Simonucci, C., Viollier, E., Sarazin, G., Prévot, F., and Jézéquel, D. (2007).
836 Benthic response to shellfish farming in Thau lagoon: Pore water signature. *Estuarine, Coastal*
837 *and Shelf Science* 72, 406–419. doi: 10.1016/j.ecss.2006.11.011.
- 838 Meysman, F. J. R., Risgaard-Petersen, N., Malkin, S. Y., and Nielsen, L. P. (2015). The
839 geochemical fingerprint of microbial long-distance electron transport in the seafloor.
840 *Geochimica et Cosmochimica Acta* 152, 122–142. doi: 10.1016/j.gca.2014.12.014.
- 841 Michaud, E., Aller, R., Zhu, Q., Heilbrun, C., and Stora, G.: Density and size-dependent
842 bioturbation effects of the infaunal polychaete *Nephtys incisa* on sediment biogeochemistry
843 and solute exchange, *Journal of marine research*, 79, 181,
844 <https://doi.org/10.1357/002224021834670801>, 2021.
- 845 Middelburg, J. J., Soetaert, K., and Hagens, M.: Ocean Alkalinity, Buffering and
846 Biogeochemical Processes, *Reviews of Geophysics*, 58, e2019RG000681,
847 <https://doi.org/10.1029/2019RG000681>, 2020.
- 848 Mojtahid, M., Depuydt, P., Mouret, A., Le Houedec, S., Fiorini, S., Chollet, S., Massol, F.,
849 Dohou, F., Filipsson, H. L., Boer, W., Reichart, G.-J., and Barras, C.: Assessing the impact of
850 different carbonate system parameters on benthic foraminifera from controlled growth
851 experiments, *Chemical Geology*, 623, 121396,
852 <https://doi.org/10.1016/j.chemgeo.2023.121396>, 2023.
- 853 Murray, J. W. (2006). *Ecology and Applications of Benthic Foraminifera*. Cambridge University
854 Press.
- 855 Nielsen, L. P., Risgaard-Petersen, N., Fossing, H., Christensen, P. B., and Sayama, M. (2010).
856 Electric currents couple spatially separated biogeochemical processes in marine sediment.
857 *Nature* 463, 1071–1074. doi: 10.1038/nature08790.
- 858 O'Brien, P. A. J., Polovodova Asteman, I., and Bouchet, V. M. P. (2021). Benthic Foraminiferal
859 Indices and Environmental Quality Assessment of Transitional Waters: A Review of Current
860 Challenges and Future Research Perspectives. *Water* 13, 1898. doi: 10.3390/w13141898.

861 Office Français De La Biodiversité Découvrir Les Estuaires de La Façade Manche/Atlantique
862 | Le Portail Technique De l'OFB. Available online: <https://professionnels.ofb.fr/fr/node/276>
863 (accessed on 29 Novembre 2023).

864 Patterson, R. T., and Fishbein, E. (1989). Re-examination of the statistical methods used to
865 determine the number of point counts needed for micropaleontological quantitative research.
866 *J. Paleontol.* 63, 245–248. doi: 10.1017/S0022336000019272.

867 Petersen, J., Barras, C., Bézos, A., La, C., de Nooijer, L. J., Meysman, F. J. R., Mouret, A.,
868 Slomp, C. P., and Jorissen, F. J.: Mn/Ca intra- and inter-test variability in the benthic foraminifer
869 *Ammonia tepida*, *Biogeosciences*, 15, 331–348, <https://doi.org/10.5194/bg-15-331-2018>,
870 2018.

871 Pfeffer, C., Larsen, S., Song, J., Dong, M., Besenbacher, F., Meyer, R. L., et al. (2012).
872 Filamentous bacteria transport electrons over centimetre distances. *Nature* 491, 218–221. doi:
873 10.1038/nature11586.

874 Polovodova, I., and Schonfeld, J. (2008). Foraminiferal Test Abnormalities in the Western
875 Baltic Sea. *The Journal of Foraminiferal Research* 38, 318–336. doi: 10.2113/gsjfr.38.4.318.

876 Pucci, F., Geslin, E., Barras, C., Morigi, C., Sabbatini, A., Negri, A., et al. (2009). Survival of
877 benthic foraminifera under hypoxic conditions: Results of an experimental study using the
878 CellTracker Green method. *Marine Pollution Bulletin* 59, 336–351. doi:
879 10.1016/j.marpolbul.2009.08.015.

880 R Core Team (2022). R: A language and environment for statistical computing. R Foundation
881 for Statistical Computing, Vienna, Austria. URL <https://www.R-project.org/>

882 Rao, A. M. F., Malkin, S. Y., Hidalgo-Martinez, S., and Meysman, F. J. R. (2016). The impact
883 of electrogenic sulfide oxidation on elemental cycling and solute fluxes in coastal sediment.
884 *Geochimica et Cosmochimica Acta* 172, 265–286. doi: 10.1016/j.gca.2015.09.014.

885 Réseau SYVEL Système de veille dans l'estuaire de la Loire GIP Loire Estuaire,
886 <https://www.loire-estuaire.org/dif/do/init> (assessed on 29 Novembre 2023)

887 Revsbech, N. P., and Jørgensen, B. B. (1986). “Microelectrodes: Their Use in Microbial
888 Ecology,” in *Advances in Microbial Ecology Advances in Microbial Ecology.*, ed. K. C. Marshall
889 (Boston, MA: Springer US), 293–352. doi: 10.1007/978-1-4757-0611-6_7.

890 Revsbech, N. P. (1989). An oxygen microsensor with a guard cathode. *Limnol. Oceanogr.* 34,
891 474–478. doi: 10.4319/lo.1989.34.2.0474.

892 Richirt, J., Guihéneuf, A., Mouret, A., Schweizer, M., Slomp, C. P., and Jorissen, F. J. (2022).
893 A historical record of benthic foraminifera in seasonally anoxic Lake Grevelingen, the
894 Netherlands. *Palaeogeography, Palaeoclimatology, Palaeoecology* 599, 111057. doi:
895 10.1016/j.palaeo.2022.111057.

896 Risgaard-Petersen, N., Revil, A., Meister, P., and Nielsen, L. P. (2012). Sulfur, iron-, and
897 calcium cycling associated with natural electric currents running through marine sediment.
898 *Geochimica et Cosmochimica Acta* 92, 1–13. doi: 10.1016/j.gca.2012.05.036.

899 Risgaard-Petersen, N., Damgaard, L. R., Revil, A., and Nielsen, L. P. (2014). Mapping electron
900 sources and sinks in a marine biogeobattery. *Journal of Geophysical Research:*
901 *Biogeosciences* 119, 1475–1486. doi: 10.1002/2014JG002673.

- 902 Risgaard-Petersen, N., Kristiansen, M., Frederiksen, R. B., Dittmer, A. L., Bjerg, J. T., Trojan,
903 D., et al. (2015). Cable Bacteria in Freshwater Sediments. *Appl Environ Microbiol* 81, 6003–
904 6011. doi: 10.1128/AEM.01064-15.
- 905 Schönfeld, J., and Mendes, I. (2022). Benthic foraminifera and pore water carbonate chemistry
906 on a tidal flat and salt marsh at Ria Formosa, Algarve, Portugal. *Estuarine, Coastal and Shelf*
907 *Science* 276, 108003. doi: 10.1016/j.ecss.2022.108003.
- 908 Scott, D. B., Medioli, F. S., and Schafer, C. T.: Monitoring in Coastal Environments Using
909 Foraminifera and Thecamoebian Indicators, Cambridge University Press, 193 pp., 2007.
- 910 Seitaj, D., Schauer, R., Sulu-Gambari, F., Hidalgo-Martinez, S., Malkin, S. Y., Burdorf, L. D.
911 W., et al. (2015). Cable bacteria generate a firewall against euxinia in seasonally hypoxic
912 basins. *Proc Natl Acad Sci USA* 112, 13278–13283. doi: 10.1073/pnas.1510152112.
- 913 Soetaert, K., Hofmann, A. F., Middelburg, J. J., Meysman, F. J. R., and Greenwood, J. (2007).
914 The effect of biogeochemical processes on pH. *Marine Chemistry* 105, 30–51. doi:
915 10.1016/j.marchem.2006.12.012.
- 916 Thibault de Chanvalon, A., Metzger, E., Mouret, A., Cesbron, F., Knoery, J., Rozuel, E., et al.
917 (2015). Two-dimensional distribution of living benthic foraminifera in anoxic sediment layers of
918 an estuarine mudflat (Loire Estuary, France). *Biogeochemistry: Sediment* doi: 10.5194/bg-
919 12-10311-2015.
- 920 Thibault de Chanvalon, A., Metzger, E., Mouret, A., Knoery, J., Chiffolleau, J.-F., and Brach-
921 Papa, C. (2016a). Particles transformation in estuaries: Fe, Mn and REE signatures through
922 the Loire Estuary. *Journal of Sea Research* 118, 103–112. doi: 10.1016/j.seares.2016.11.004.
- 923 Thibault de Chanvalon, A., Mouret, A., Knoery, J., Geslin, E., Péron, O., and Metzger, E.
924 (2016b). Manganese, iron and phosphorus cycling in an estuarine mudflat, Loire, France.
925 *Journal of Sea Research* 118, 92–102. doi: 10.1016/j.seares.2016.10.004.
- 926 Thibault de Chanvalon, A., Metzger, E., Mouret, A., Knoery, J., Geslin, E., and Meysman, F.
927 J. R. (2017). Two dimensional mapping of iron release in marine sediments at submillimetre
928 scale. *Marine Chemistry* 191, 34–49. doi: 10.1016/j.marchem.2016.04.003.
- 929 Thibault de Chanvalon, A., Geslin, E., Mojtahid, M., Métais, I., Méléder, V., and Metzger, E.
930 (2022). Multiscale analysis of living benthic foraminiferal heterogeneity: Ecological advances
931 from an intertidal mudflat (Loire estuary, France). *Continental Shelf Research* 232, 104627.
932 doi: 10.1016/j.csr.2021.104627.
- 933 Toyofuku, T., Matsuo, M. Y., de Nooijer, L. J., Nagai, Y., Kawada, S., Fujita, K., et al. (2017).
934 Proton pumping accompanies calcification in foraminifera. *Nat Commun* 8, 14145. doi:
935 10.1038/ncomms14145.
- 936 van Cappellen, P., and Wang, Y. (1996). Cycling of iron and manganese in surface sediments:
937 A general theory for the coupled transport and reaction of carbon, oxygen, nitrogen, sulfur,
938 iron, and manganese. *American Journal of Science* 296, 197–243.
- 939 van de Velde, S., Lesven, L., Burdorf, L. D. W., Hidalgo-Martinez, S., Geelhoed, J. S., Van
940 Rijswijk, P., et al. (2016). The impact of electrogenic sulfur oxidation on the biogeochemistry
941 of coastal sediments: A field study. *Geochimica et Cosmochimica Acta* 194, 211–232. doi:
942 10.1016/j.gca.2016.08.038.
- 943 World Register of Marine Species. Available online:
944 <https://www.marinespecies.org/index.php> (assessed on 05 May 2022).

	D e p t h l a y e r	La y e r v o l u m e (c m ⁻³)	<i>Hay nesi na ger mani ca</i>	<i>Am mon ia</i> spp.	Elph idiu m spp.	<i>Quinqu eloculin a</i> spp.	<i>DS- 5</i> spe cim en	<i>Ammob aculites aggluti nans</i>	Other agglu tinan s	T o t al	C / T r a t i o	D S - 5 / C r a t i o	
S t 1	[0-2 mm]	10.6	179	113	18	2	0	23	9	344	0.91	0.00	
	[2-4 mm]	10.6	42	18	6	0	0	5	7	78	0.85	0.00	
	[4-6 mm]	10.6	26	4	0	0	0	3	0	33	0.91	0.00	
	[6-8 mm]	10.6	28	9	1	0	0	3	0	41	0.93	0.00	
	[8-10 mm]	10.6	15	5	0	0	0	3	2	25	0.80	0.00	
	[10- 12 mm]	10.6	26	5	0	0	0	4	4	39	0.79	0.00	
	[12- 14 mm]	10.6	23	1	0	0	0	4	2	30	0.80	0.00	
	[14- 16 mm]	10.6	15	5	0	0	0	4	1	25	0.80	0.00	
	[16- 18 mm]	10.6	25	3	1	0	0	9	2	40	0.73	0.00	
	[18- 20 mm]	10.6	12	4	1	0	0	3	0	20	0.85	0.00	
	[20- 30 mm]	52.8	110	61	2	0	0	77	6	256	0.68	0.00	
	[30- 40 mm]	52.8	99	67	11	0	2	57	9	245	0.73	0.01	
	[40- 50 mm]	52.8	93	42	2	0	0	28	4	169	0.81	0.00	
	S t 2	[0-2 mm]	10.6	95	37	9	3	1	4	0	149	0.97	0.01
		[2-4 mm]	10.6	38	18	1	0	2	1	1	61	0.97	0.03
[4-6 mm]		10.6	24	8	2	0	0	5	0	39	0.87	0.00	
[6-8 mm]		10.6	4	7	0	0	2	6	1	20	0.65	0.15	
[8-10 mm]		10.6	8	0	0	0	1	3	0	12	0.75	0.11	
[10- 12 mm]		10.6	6	0	0	0	1	7	3	17	0.41	0.14	
[12- 14 mm]		10.6	11	2	0	0	0	10	2	25	0.52	0.00	

[14-16 mm]	10.6	0	0	0	0	2	13	1	16	0.13	1.00
[16-18 mm]	10.6	16	0	0	0	4	17	2	39	0.51	0.20
[18-20 mm]	10.6	31	1	0	0	3	15	0	50	0.70	0.09
[20-30 mm]	52.8	22	6	2	0	20	33	6	89	0.56	0.40
[30-40 mm]	52.8	15	5	0	0	4	5	8	37	0.65	0.17
[40-50 mm]	52.8	9	0	0	0	10	5	1	25	0.76	0.53

S t 3	[0-2 mm]	10.6	238	52	19	83	0	8	5	405	0.97	0.00
	[2-4 mm]	10.6	91	11	5	8	0	7	2	124	0.93	0.00
	[4-6 mm]	10.6	148	9	4	4	2	4	2	173	0.97	0.01
	[6-8 mm]	10.6	133	4	3	1	3	6	1	151	0.95	0.02
	[8-10 mm]	10.6	73	2	2	0	2	6	1	86	0.92	0.03
	[10-12 mm]	10.6	55	2	1	0	2	1	1	62	0.97	0.03
	[12-14 mm]	10.6	60	1	2	0	3	8	1	75	0.88	0.05
	[14-16 mm]	10.6	37	6	3	0	7	3	2	58	0.91	0.13
	[16-18 mm]	10.6	21	2	0	0	5	5	2	35	0.80	0.18
	[18-20 mm]	10.6	18	4	1	0	5	5	6	39	0.72	0.18
	[20-30 mm]	52.8	38	4	0	0	21	20	16	99	0.64	0.33
	[30-40 mm]	52.8	7	4	1	0	35	15	19	81	0.58	0.74
	[40-50 mm]	52.8	8	9	1	0	57	15	32	122	0.61	0.76